MINISTRY OF AVIATION

AERONAUTICAL RESEARCH COUNCIL

CURRENT PAPERS

Measurements of Buffeting on Slender Wing Models

by

D. G. Mabey, M.Sc.(Eng.)

LONDON· HER MAJESTY'S STATIONERY OFFICE

1967

TEN SHILLINGS NET

U.D.C. No. 533.6.013.43 : 533.693.3 : 532.527 : 533.6.011.32/34

C.P. No.917*
March 1966

MEASUREMENTS OF BUFFETING ON SLENDER WING MODELS

by

D. G. Mabey, M.Sc.(Eng.)

SUMMARY

Tests on two solid slender wing models show that there are two stages in the wing buffeting at subsonic speeds;

(1) a mild buffeting due to leading-edge vortices, and
(2) a severe buffeting at vortex breakdown.

At supersonic speeds the mild buffeting is weaker, probably because of the reduced size and intensity of the leading-edge vortices.

Tests on two aeroelastic models at subsonic speeds show that the mild buffeting is principally at the wing 3rd or higher distortion modes. The order of magnitude of this buffeting suggests that on a supersonic transport aircraft this might be perceptible during subsonic climb-out at high EAS.

*Replaces R.A.E. Tech. Report No.66086 - A.R.C.27923.

CONTENTS

1 INTRODUCTION

The flow at incidence over slender wing aircraft with sharp leading-edges is dominated by a pair of vortices which strongly influence the aircraft loadings. The effect of the vortices on the steady loads is well known[1]. However the effect on buffet* characteristics is uncertain, although significant pressure fluctuations have been measured under the leading-edge vortices[2]. No wing buffeting has been reported on the low speed HP.115 but a very light buffeting has been reported on the high speed Bristol 221 at subsonic speeds.

The present wind tunnel tests, on two solid models (Models 1 and 2) were made to investigate the basic nature of slender wing buffeting. The measurements consisted of the variation of unsteady wing-root stress with incidence. Using this method two separate stages of wing buffeting were identified,

(1) a mild buffeting associated with the existence of leading-edge vortices, and

(2) a strong buffeting following vortex breakdown[3].

Accurate measurements of buffeting on solid wind tunnel models are difficult because the models normally have unrepresentative aerodynamic and structural damping coefficients and unrepresentative distortion modes. Hence the two aeroelastic models (Models 3 and 4) were also tested.

This report presents buffeting measurements on all four wings and briefly discusses their possible implications.

2 EXPERIMENTAL DETAILS

2.1 Models

Buffeting measurements were made on four slender wing models constructed for other static and dynamic tests during the evolution of a supersonic transport design. The external shapes of these models differ significantly from the Concord prototype and production aircraft.

Fig.1 shows the general arrangement of Model 1. This is a 1/75 scale solid bronze model of an early supersonic transport design. Four semi-conductor strain gauges at the wing-root were wired so that the signals from the port and starboard wings were additive for symmetric deformations of the model, while signals resulting from antisymmetric deformations were virtually eliminated. Before the buffeting tests the model was ground resonance tested on its supporting sting. Identified symmetric distortion modes are shown in Fig.2. The

*Throughout this report buffet will be defined as the applied aerodynamic excitation and buffeting as the structural response. The sensitive semiconductor strain gauges used on these models are probably able to detect buffeting which would be imperceptible to passengers.

wind-off structural damping is low in both of these modes because of the solid model construction.

Fig.3 shows the general arrangement of Model 2. This is a 1/30 scale solid steel model of a supersonic transport design. Model 2 was fitted with four strain gauges on the port wing so that symmetric and antisymmetric deformations would produce a signal. Distortion modes identified in a ground resonance test are shown in Fig.4.

Fig.5 shows a photograph of Model 3, which is generally similar in external shape to Models 1 and 2. This is a 1/55 scale flutter model of an early supersonic transport design. The aircraft skin, spars and ribs are represented by etching from light alloy; the volume within the model is stabilised with expanded plastic foam. The model could be mounted on its flutter excitation support so that total damping measurements (wind on) could be made after the buffeting measurements.

Wire strain gauges were provided on this model for flutter tests with only two active gauges in each bridge at the port tip and at the port wing-root so that both symmetric and antisymmetric deformations would produce a signal as on Model 2. (Semi-conductor strain gauges would have been preferred but could not be applied without altering the model inertias.) Some symmetric and antisymmetric distortion modes are shown in Fig.6. (The frequencies measured in the initial ground resonance test are slightly different from those subsequently measured in the tunnel because of small differences in the support and excitation systems.) The wind-off structural damping is higher than on Models 1 and 2 and more typical of probable full scale values.

Fig.7 shows the general arrangement of Model 4. This is a deformation model of an early supersonic transport design. The model construction was similar to that of Model 3 and the model was mounted on a solid sting. Semiconductor strain gauges were applied directly to the outside skin of this deformation model (where the inertia distributions were not critical) and then covered with a thin araldite fairing. Two bridges, each with four active gauges were provided near the wing-root and at 50% semi-span as shown in Fig.7. The gauges were wired to add the port and starboard signals as on Model 1. The approximate distortion modes which appeared in the buffet signals are shown in Fig.8. The total damping (wind on) could not be measured because no provision was made for exciting this model.

It should be noted that the "full scale" frequencies of Figs.2, 4 and 8 are simply obtained by multiplying the model frequencies by the model scale, and are not directly related to a specific aircraft. The values for Model 3 are, of course, related to a specific aircraft.

2.2 Measurements

The rms wing buffeting signals on all four wings were measured on a spectrum analyser (the tuned signals were measured with 6% bandwidth). To avoid overstressing models 3 and 4 (9 and 30 lb maximum lift respectively) the steady lift and pitching moment at every kinetic pressure were monitored before the buffeting tests.

The total damping measurements on Model 3 were derived from vector plots of model response to mechanical excitation at particular frequencies.

2.3 Test conditions

The models were tested in either the 13 x 9 ft (low speed) or the 3 x 3 ft (subsonic/transonic/supersonic) wind tunnel. Table 1 gives the test conditions. The low Reynolds number of the Model 3 and 4 tests will be noted. Ballotini (small glass spheres) were applied in narrow bands to fix transition on Models 1, 2 and 4 but not on Model 3 (to avoid altering the model inertia distributions).

3 RESULTS

3.1 Model 1

Model 1 was first briefly tested in the 3 ft tunnel and a mild buffeting was detected at about 6° incidence (α) at all Mach numbers (M) from 0.40 to 0.80. Above M=0.80 this mild buffeting was not detected over the increased signal arising from tunnel unsteadiness. Oil flow photographs (Fig.9) show that this buffeting is associated with the existence of the leading-edge primary vortex. Owing to some asymmetry this vortex appears first on the port wing at $\alpha = 6^{\circ}$ (Fig. 9(a)). As incidence increases to $\alpha = 7^{\circ}$ there is an intermediate flow with several spanwise vortices near both tips (Fig. 9(b)). At $\alpha = 8^{\circ}$ these vortices have combined to form one single vortex on the port wing; there are still two vortices on the starboard wing (Fig. 9(c)).

Model 1 could not be tested at incidences much higher than $\alpha = 14^{\circ}$ in the 3 ft tunnel because of excessive blockage, even in the 36 x 26 in slotted working section. Hence the tests were extended to the 13 x 9 ft low speed wind tunnel, where blockage effects would be insignificant even at $\alpha = 30^{\circ}$.

Fig.10 shows the variation of total wing-root strain signal from $\alpha = 1^{\circ}$ to $\alpha = 30^{\circ}$ in the 13 x 9 ft tunnel*. The curve comprises several different sections which are related with the flow development. From $\alpha = 1^{\circ}$ to $\alpha = 6^{\circ}$ there is a constant signal owing to the flow unsteadiness induced by the support and the support vibration**. Then from $\alpha = 6^{\circ}$ to $\alpha = 10^{\circ}$ the signal builds up steadily as the leading-edge vortices develop. From $\alpha = 10^{\circ}$ to $\alpha = 22.5^{\circ}$ there is a constant signal implying "a plateau" in the buffeting. From $\alpha = 22.5^{\circ}$ to $\alpha = 26^{\circ}$ the signal builds up rapidly as the vortex breakdown point, clearly visible by condensation in the vortex core, moves upstream from the trailing-edge on to the port wing. From $\alpha = 26^{\circ}$ to $\alpha = 29^{\circ}$ there is a further sudden build up of signal which must have been caused by vortex breakdown on the starboard wing. This vortex breakdown was not shown by condensation in the core, probably because the core was larger than for the port wing. From $\alpha = 29^{\circ}$ to 30° the buffeting falls rapidly.

The wing buffeting was next examined in more detail by measuring its response when tuned to the frequency of the distortion modes. Fig.11 shows the variation of tuned wing-root strain signal with incidence. The major portion of the buffeting at vortex breakdown is clearly associated with the wing response at its fundamental frequency of 300 c/s (Fig. 11(a)). (This response may come from a larger low frequency component in the excitation or to the larger scale of the disturbance.) The fundamental mode is not significantly excited by the formation of the leading-edge vortex; most of the response from $\alpha = 6^{\circ}$ to $\alpha = 10^{\circ}$ comes from the third deformation mode at 700 c/s (Fig.11(b)). This mode is also excited by vortex breakdown, but not as strongly as the fundamental mode. A mode at 1330 c/s was also weakly excited by both vortex formation and vortex breakdown (Fig.11(c)).

Sideslip significantly lowers the incidence for vortex breakdown; the vortex breaks down first in the leading wing on which the sweepback is reduced. Thus at $\pm 10^{\circ}$ sideslip (possible limiting values for cross wind landings), vortex breakdown occurs at about 15° incidence (Fig.12).

Model 1 was then tested again in the 3 ft tunnel to investigate buffeting over a wide range of density at subsonic and supersonic speeds.

---

* This test was made in two stages, from $\alpha = 1^{\circ}$ to 6° and then from $\alpha = 6^{\circ}$ because of the support geometry.

** Subsequent experience with Model 4 showed that this relatively high signal was associated with the unsteadiness produced by the bluff model support, rather than the tunnel unsteadiness, which was very low.

The tests at M = 0.50 clearly showed that buffeting could be detected (Fig.13) at stream densities as low as $\rho = 0.0091$ lb/ft^3 (a tunnel total pressure of 4 in Hg absolute). Hence buffeting tests at this density on Model 3 (a fragile aeroelastic model) would be possible if the dampings on both models were comparable. The sensitivity of the semi-conductor wing-root strain gauge bridge on Model 1 was only twice that of the wire strain gauge bridge of Model 3 because Model 1 was much stiffer than Model 3. An interesting feature of these results not noticed in the previous tests was the small peak in the signal at $\alpha = 7.5^\circ$. A corresponding peak was subsequently found on Model 3 at 7.0° incidence (3.3).

Another interesting feature of these results is that at the higher kinetic pressures the wing fundamental mode at 300 c/s was excited by the mild buffeting on vortex formation (Fig.14). The other modes at 700 and 1300 c/s were also excited together with an additional mode at 1920 c/s. Although the particular modes detected depend critically on the somewhat arbitrary position of the strain gauges, excitation of modes over this frequency range suggests that the excitation spectrum associated with the formation of the leading-edge vortex is relatively flat for values of $\omega\bar{c}/v$ from 2.0 to 13.0.

The first supersonic test was made at M = 1.4, the lowest Mach number at which reflected shock waves were clear of the model. The buffeting onset was not sharply defined, except at the highest density (Fig.15). However there was a signal peak at $\alpha = 8^\circ$ which recalls that at $\alpha = 7^\circ$, M = 0.50, (Fig.13). A vapour screen[5] in the working section revealed an upper surface vortex at incidences higher than 7°. No vortex instability was apparent in the vapour screen at $\alpha = 8^\circ$.

Fig.15 also shows that the "plateau" level of buffeting is not much higher than the signal at zero incidence. The buffeting at supersonic speeds is probably less than at subsonic speeds because the leading-edge vortices are weaker. (The leading-edge vortices develop much less non-linear lift at supersonic speeds; see e.g. Ref.6.) The leading-edge vortices are also much smaller at supersonic speeds as Fig.33 of Ref.7 clearly demonstrates.

Tests at M = 1.6 were inconclusive. The signal at zero incidence was much higher (probably because of quadrant vibration excited by the tunnel shock) and no signal peak was detected.

3.2 Model 2

In broad outline the buffeting characteristic of Model 2 (Fig.16) resemble those of Model 1 (Fig.10). On Model 2 the existence of a vortex is apparent at $\alpha = 5^{\circ}$, there is a small signal peak at $\alpha = 8^{\circ}$ and a "plateau" in the signal from $\alpha = 12^{\circ}$ to $\alpha = 21^{\circ}$. Vortex breakdown reaches the trailing edge of the starboard wing at $\alpha = 23^{\circ}$ and the port wing at $\alpha = 26^{\circ}$*.

The wing fundamental mode is strongly excited (Fig.17(a)) and the second distortion mode is also excited (Fig.17(b)). The third distortion mode is weakly excited and its signal actually falls from $\alpha = 0^{\circ}$ to $\alpha = 6^{\circ}$ (Fig.17(c)). The total signal shows a similar fall (Fig.16) and this could be associated with the suppression of the lower surface vortex as the incidence is increased from 0° to 6°.

The effects of sideslip on the incidence for vortex breakdown were similar to those in Model 1 (Fig.12) and are not presented here. A full account of the tests in Model 2, including a comparison of wing-root buffeting signals and static pressure fluctuations measured under the vortex, will be presented in a separate report[8].

3.3 Model 3

Since Model 3 had a representative structure the safe limits for lift and pitching moment were far less than for the solid models. Safe limits of lift and pitching moment (based on a factor of safety of 3) were estimated and rigorously applied. The earlier results from Model 1 (3.1) suggested that the interesting incidence range would be from $\alpha = 6^{\circ}$ (buffeting onset) to $\alpha = 12^{\circ}$ (the buffeting plateau). To attain this incidence range the kinetic pressure was severely restricted. In the low speed 13 x 9 ft tunnel operating at atmospheric density the maximum velocity was only 150 ft/s. In the 3 x 3 ft tunnel the free-stream density could be reduced and hence the velocity increased for the same kinetic pressures.

In the 13 x 9 ft tunnel no buffeting could be detected above the relatively high signal at zero incidence. In the 3 ft tunnel the buffeting measurements were made at M = 0.50 and free stream densities of 0.0048 and 0.0096 lb/ft^3 (equivalent to 80 and 115 knots EAS).

---

* Model shaking prevented tests at higher incidence at the test speed of 252 ft/s. The step in the buffeting signal between vortex breakdown on the port and starboard wings on Model 1 (Fig.10) was not observed on Model 2.

Fig.18(a) shows typical plots of the variation of total tip strain signal with incidence at M = 0.50. Buffeting onset is at $\alpha = 5^{\circ}$ and 4° at $\rho = 0.0048$ and 0.0096 lb/ft^3 respectively. At both densities there is a peak in the signal near $\alpha = 7^{\circ}$, similar to that at $\alpha = 8^{\circ}$ on Model 1. Even at the lowest density the maximum incidence was restricted to $\alpha = 9^{\circ}$ and so the existence of the buffeting plateau was not established. Fig.18(b) shows the data corrected for electrical pick up and tunnel unsteadiness. It is assumed that there is no correlation between the buffeting signal and the signal at zero incidence, i.e. $\sigma_B = \sqrt{\sigma_T^2 - \sigma_o^2}$.

Fig.19 shows that the tip buffeting is proportional to ρ rather than $(\rho)^{\frac{1}{2}}$, which implies the predominance of structural damping over aerodynamic damping[9,10]. The predominance of structural damping on solid wind tunnel models has been noticed in previous buffet tests but the predominance of structural damping on this aeroelastic model was not expected. However, an examination of the spectra of the tip strain signal Fig.20 shows the interesting fact that most of the buffeting is at 3rd symmetric distortion mode at 273 c/s and not at the 1st symmetric distortion mode as on unswept wings. (Fig.20 shows that the 3rd symmetric distortion mode predominates even in the smaller wing-root strain signal.) Direct measurements show little increase in total damping with stream density for the 3rd mode (Fig.21(c)). Hence structural damping must predominate for this mode. (The mode at 155 c/s could have been symmetric or antisymmetric (see Fig.6).)

At the wing fundamental frequency f = 127.5 c/s, there is a large variation in total damping with stream density (Fig.21(a)) but this mode was not sufficiently excited by the buffet to decide if either

$$TS \propto \rho \qquad (1)$$

$$\text{or } TS \propto \rho^{\frac{1}{2}} \qquad (2)$$

is appropriate.

The model and aircraft tip stresses will be identical because of the dimensional similarity relationships[11]. Tip stresses and amplitudes during subsonic climb-out are estimated in Appendix 1 and discussed in Section 4.

3.4 Model 4

Model 4 was tested to determine how buffeting varied with velocity and density for the different vibration modes. In the low speed 13 x 9 ft tunnel tests at atmospheric density were frustrated by Reynolds number effects, e.g.

as the tunnel velocity increased from 175 to 250 ft/s the incidence for vortex formation fell from $\alpha = 8^{\circ}$ to 6°. In the 3 ft tunnel, tests at a constant low density ($\rho = 0.005$ lb/ft^3) over a speed range from M = 0.30 to 0.70 were also unsuccessful. If the tunnel kinetic pressure is increased by increasing the speed, rather than the free stream density, the frequency parameter $\omega\bar{c}/v$ is reduced. Any change in frequency parameter is really undesirable, even if the excitation spectrum is relatively flat, as it is in these tests. However tests at a constant speed M = 0.40, over a 4/1 range of density, yielded some interesting data.

Fig.22 attempts to reduce the buffeting measurements by both equations (1) and (2) above. The arbitrary scales used have been adjusted so that points for the highest density are common to both equations.

Data are provided for the three modes excited. The fundamental mode at f = 263 c/s is not very strongly excited (cf the WRS spectra for Model 3 shown in Fig.20)). However careful examination suggests that the buffeting data for this mode do appear to fit equation (2), rather than equation (1), implying that aerodynamic damping predominates over structural damping (cf the contribution of aerodynamic damping to the total damping for the fundamental mode on Model 3, Fig.21(a)). The second mode at f = 380 c/s is strongly excited, but the data are inconclusive (Fig.22(b)). The response of this mode is probably limited by a mixture of aerodynamic and structural damping. The third mode at f = 1470 c/s is fairly strongly excited but structural damping obviously predominates (Fig.22(c)).

It is worth noting that the model response over this frequency range again implies that the spectrum of excitation from the leading-edge vortex is relatively flat in the range of $\omega\bar{c}/v$ from 2.5 to 13.5 as on Model 1.

4 DISCUSSION

Tests on the solid models 1 and 2 indicate that slender wings can respond to the buffet excitations provided by leading-edge vortices and vortex breakdown at subsonic speeds up to M = 0.80. The more important problem is to determine if the aircraft response would be signficant. To answer this question, even on an unswept wing[4], aeroelastic models must be tested because the mode shapes, frequencies and total dampings are then appropriate to the aircraft. This is particularly important for buffeting tests on slender wings, where higher modes than the fundamental are most strongly excited (note the large differences between the 3rd mode shapes and frequencies for the solid models and the aeroelastic models which have similar external geometry).

Measurements on the aeroelastic Model 3 (Appendix A) show that the full scale tip amplitude at 7° incidence and 270 knots EAS would be about ±0.3 inch at 5 c/s. (These figures are estimated after applying very large scaling factors and ignore any change in mode shape between 0 and 270 knots EAS.) Because the model was supported at the centre of the fuselage, amplitudes and accelerations of the aircraft fuselage cannot be directly estimated. However, any buffeting above 0.02g might be considered uncomfortable[12]. Hence, during the subsonic climb after take-off to about 5000 ft altitude, there will be a short period when the combination of incidence and EAS will be such that buffeting induced by the leading edge vortices might be detected. The tests on Model 3 can only give the probable order of magnitude of buffeting on a typical slender wing aircraft.

The normal flight envelope of a slender wing aircraft is unlikely to extend into the vortex breakdown region so that the buffeting induced by vortex breakdown is rather academic. However, it is interesting to recall that vortex breakdown did excite the wing fundamental mode on Models 1 and 2. Models 3 and 4 could not be tested at the incidences required for vortex breakdown. Tests of three identical 65° delta wing made respectively of steel, light alloy and magnesium should provide data to substantiate the buffeting scale relationships appropriate for vortex breakdown[13].

These present tests give no information about the pressure fluctuations exciting the buffeting apart from showing that the buffet excitation spectrum is relatively flat over the frequency range from

$$2 < \omega\bar{c}/v < 12 \quad .$$

Typical pressure fluctuation measurements[8] on Model 2 on the WRS plateau at $\alpha = 12°$ show

$$\Delta\bar{p}/q = 0.02$$

and at vortex breakdown $\alpha = 24°$

$$\Delta\bar{p}/q = 0.07 \quad .$$

A more detailed study of pressure fluctuations on slender wings to extend the measurements of Wyatt and Owen[14] seems desirable. In particular the planned (1966) flight comparison of pressure fluctuations measured on the FD2 and the Bristol 221 might reveal any basic differences in vortex structure owing to planform changes or to the change from a round to a sharp leading-edge. (The occasional mild buffeting on the Bristol 221 reported by pilots does not by itself prove that the pressure fluctuations under the vortex are smaller than on the FD2. The structure of the 221 is different from that of the FD2 and the pilot sits 6 ft further forward.)

A final question concerns possible Reynolds number effects on the buffeting characteristics of slender wings. With sharp leading-edges to fix separation lines Reynolds number effects on the developed vortex flow should be much smaller than on wings with round leading-edges (there is certainly a large Reynolds number effect on the vortex on the FD2 aircraft with round leading-edges[15]). However Reynolds number effects might be significant when the small streamwise vortices are rolling up to form the main vortex (Fig.9), although no Reynolds number effects are apparent in this region on Model 1 in the 3 ft tunnel as Reynolds number increased from $0.23.10^6$ to $2.66.10^6$ (Fig.13). Again, removal of the roughness bands on the wing and nose of Model 1 in the 13 x 9 ft tunnel did not alter the incidence for vortex formation or vortex breakdown, or the buffeting. Hence the present measurements should give a fair indication of both the character and order of magnitude of the buffeting on full scale slender wing aircraft.

5 CONCLUSIONS

Tests on two solid slender wing models show that there are two stages in the wing buffeting at subsonic speeds (Figs.10 and 16):-

(1) a mild buffeting when the leading-edge vortices are fully established, and (2) a severe buffet at vortex breakdown.

At supersonic speeds the mild buffeting is weaker, probably because of the reduced size and intensity of the leading-edge vortices.

Tests on two aeroelastic models show that the mild buffeting is principally at the wing 3rd distortion mode (Fig.20). The order of magnitude of this buffeting suggests that on a supersonic transport aircraft buffeting or rough vibration might be noticed during a small part of the subsonic climb-out after take-off.

ACKNOWLEDGEMENT

The author is grateful to Mr. L. Martin of the Dynamic Test Section B.A.C. Filton, for all the measurements of mode shapes and damping factors and also for the ground resonance test of Model 3.

Appendix A

TIP BUFFET STRESSES AND AMPLITUDES

The stress induced by the wing buffet on Model 3 is

$$\sigma = E(1/\lambda)\ (\Delta R/R)\ 2 \qquad (3)$$

where σ = stress lb/in^2
E = Youngs modulus lb/in^2 (1.10^7 for light alloy)
λ = gauge factor (2 for wire gauges)
ΔR = resistance change
R = resistance

(*the factor 2 is required because there are only two active gauges in the* bridge on Model 3).

Hence

$$\sigma = E(\Delta V/V) \qquad (4)$$

where ΔV = rms unsteady voltage
V = steady voltage (6.3V)

From Fig.18(b) and equation (4) the total rms stress at $\alpha = 7^\circ$ and 115 kt EAS is

$$\underline{\sigma = 65\ lb/in^2}\ .$$

Similarly from Fig.20(b) and equation (4) we have a tip stress at the third deformation mode at 273 c/s (5 c/s full scale)

$$\underline{\sigma = 40\ lb/in^2}\ .$$

In an attempt to determine the order of magnitude of the tip amplitudes associated with, but not directly related to these buffet stresses the model was subjected to a ground resonance test. The third symmetric distortion mode was excited by the normal push-rod sting used for exciting symmetric modes* and the excitation increased until the unsteady signal from the tip gauges was 26 μV

---

* This sinusoidal excitation attempts to represent the portion of the distributed "white noise" loading exciting the model. This loading takes no account of the degree of correlation of the pressure fluctuations at different points under the vortex, or of possible interactions between the response of the fairly closely spaced deformation modes.

rms (Fig.20(b)). The tip amplitude was then approximately ±0.001 inch (peak to peak) corresponding to ±0.060 inch full scale.

These stresses and deflections will increase at the higher EAS (typically about 270 knots) required during the rapid subsonic climb-out of the aircraft needed to conserve fuel. Only a small increase in total damping for the 3rd mode is suggested by extrapolation of Fig.21(c). Hence the buffet stress and deflections may be approximately increased by the ratio of the kinetic pressures, i.e. $(270/115)^2 = 5.5$.

Hence

$\sigma = 220$ lb/in^2

and the tip deflection = ±0.3 in (peak to peak)

} at 5.0 c/s full scale

Table 1

Test conditions

Model	Tunnel	Working section	Maximum Reynolds number(s) R	WRS bridge	Fundamental wing frequency c/s	$(\omega_1 c)_m/(\omega_1 c)_a$	Sting support	Date of tests
1	3 ft	Tabs M=0.40 to M=0.80	$2.66.10^6$	4 active semi-conductor gauges	285	1.65	Solid sting	October 1964
	13×9ft	low speed M=0.23	$0.92.10^6$					November 1964
	3 ft	Tabs M=0.40 to M=0.80	$2.66.10^6$					January 1965
		supersonic M=1.4 and M=1.6	$2.20.10^6$					
2	13×9ft	low speed M=0.23	$2.56.10^6$	4 active semi-conductor gauges	130	1.87	6 component balance	July 1965
3	3 ft	subsonic M=0.50	$0.34.10^6$	2 active wire gauges + 2 external resistors	127	1.00	Flutter excitation sting	January 1965
4	3 ft	subsonic M=0.40	$0.5.10^6$	4 active semi-conductor gauges	263	1.52	Solid sting	May 1965

Tabs = Top and bottom slotted section

SYMBOLS

c	damping
c_{crit}	critical damping
$\bar{c}$	average chord
EAS	equivalent airspeed knots
f	frequency c/s
$g/2$	structural damping coefficient % crit
M	Mach number
$\Delta\bar{p}$	rms pressure fluctuation lb/in^2
q	kinetic pressure $\frac{1}{2}\rho V^2$ lb/in^2
R	Reynolds number based on $\bar{c}$
V	free stream velocity ft/s
WRS	*wing-root strain*
α	incidence
β	sideslip
γ	aerodynamic damping coefficient % crit
ρ	free stream density
$\omega = 2\Pi f$	*circular frequency (radians/s)*

REFERENCES

No.	Author	Title, etc.
1	D. Küchemann	A non-linear lifting surface theory for wings of small aspect ratio with edge separations. A.R.C.17769 April 1955
2	K. G. Turner	Unpublished M.O.A. Report
3	N. Lambourne	The breakdown of certain types of vortex. A.R.C. C.P.915 September 1965
4	D. G. Mabey	Unpublished M.O.A. Report
5	I. McGregor	The vapour screen method of flow visualisation. Journ. Fluid Mech. Vol 11, p.481-511, 1961
6	L. C. Squire	Further experimental investigation of the characteristics of cambered gothic wings at Mach numbers from 0·4 to 2·0. A.R.C. R & M 3310, December 1961
7	L. C. Squire J. G. Jones A. Stanbrook	An experimental investigation of the characteristics of some plane and cambered 65° delta wings at Mach numbers from 0·7 to 2·0. A.R.C. R & M 3305, July 1961
8	R. F. Keating G. Moss	Unpublished M.O.A. Report
9	D. D. Davis Jnr W. B. Huston	The use of wind tunnels to predict flight buffet loads. NACA RM L57D25, June 1957
10	D. D. Davis Jnr D. E. Wornom	Buffet tests on an attack airplane model with emphasis on analysis of data from wind tunnel tests. NACA RM L57H13, February 1958
11	W. H. Melbourne	Aerodynamic investigation of the wind loads on a cylindrical lighthouse. Unpublished M.O.D. Report
12	H. F. Huddleston	Verbal estimates of the severity of vertical sinusoidal vibration. Unpublished work

REFERENCES (Contd)

No.	Author	Title, etc.
13	D. G. Mabey	Unpublished N.P.L. Report.
14	L. A. Wyatt T. B. Owen	Preliminary low speed measurements of skin friction and surface pressure fluctuations in a slender wing at incidence. A.R.C. 25436, September 1963
15	D. G. Mabey	Comparison of seven wing buffet boundaries measured in wind tunnels and in flight. A.R.C. C.P.840, September 1964

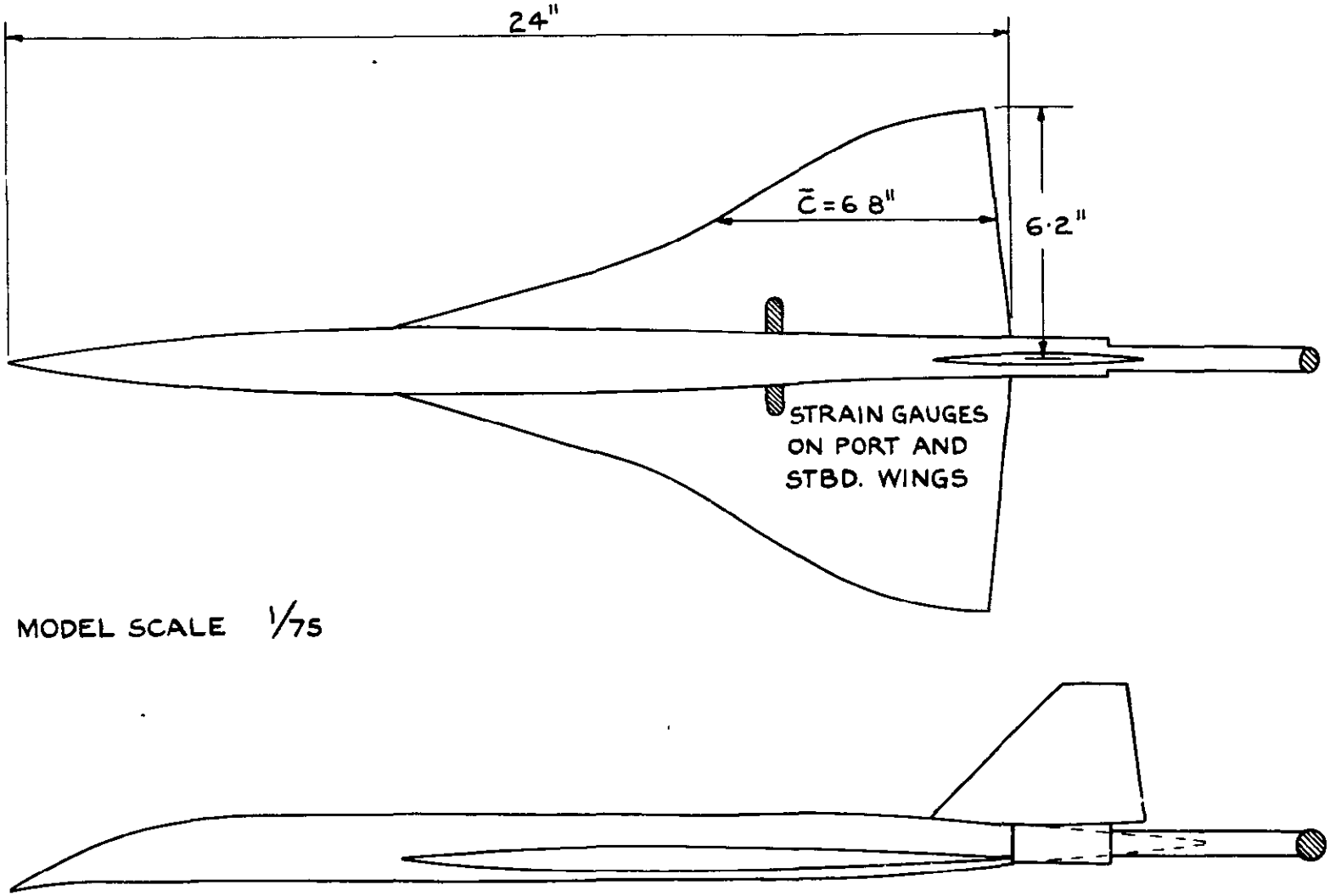

FIG.1 G.A. OF MODEL 1

(FULL SCALE FREQUENCIES IN BRACKETS)

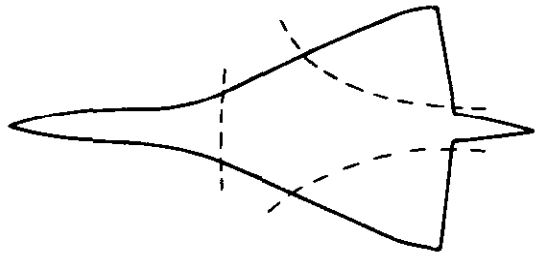

1ST DISTORTION MODE — f = 284 6 c/s (3 8 c/s); $g/2 = 0.00077$

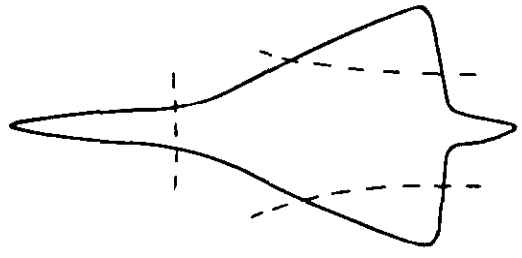

2ND DISTORTION MODE — f = 312 2 c/s (4 2 c/s); $g/2 = 0\ 0014$

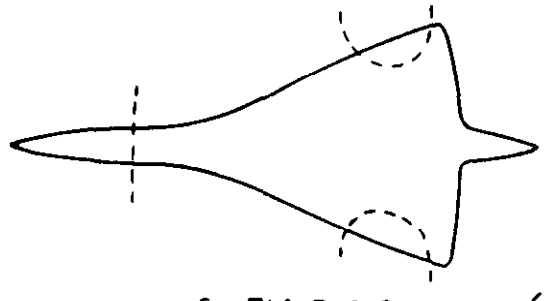

3RD DISTORTION MODE — f = 714 3 c s (9 5 c/s); $g/2 = 0\ 00078$

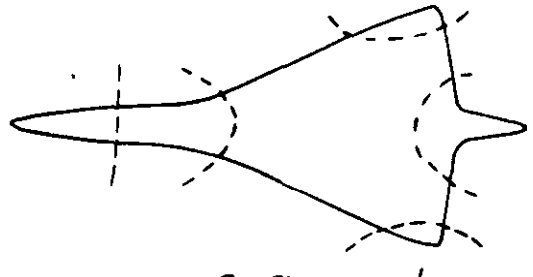

4TH DISTORTION MODE — f = 769 5 c/s (10·3 c/s); $g/2 = 0\ 0019$

FIG.2 MODEL I SYMMETRIC DISTORTION MODES

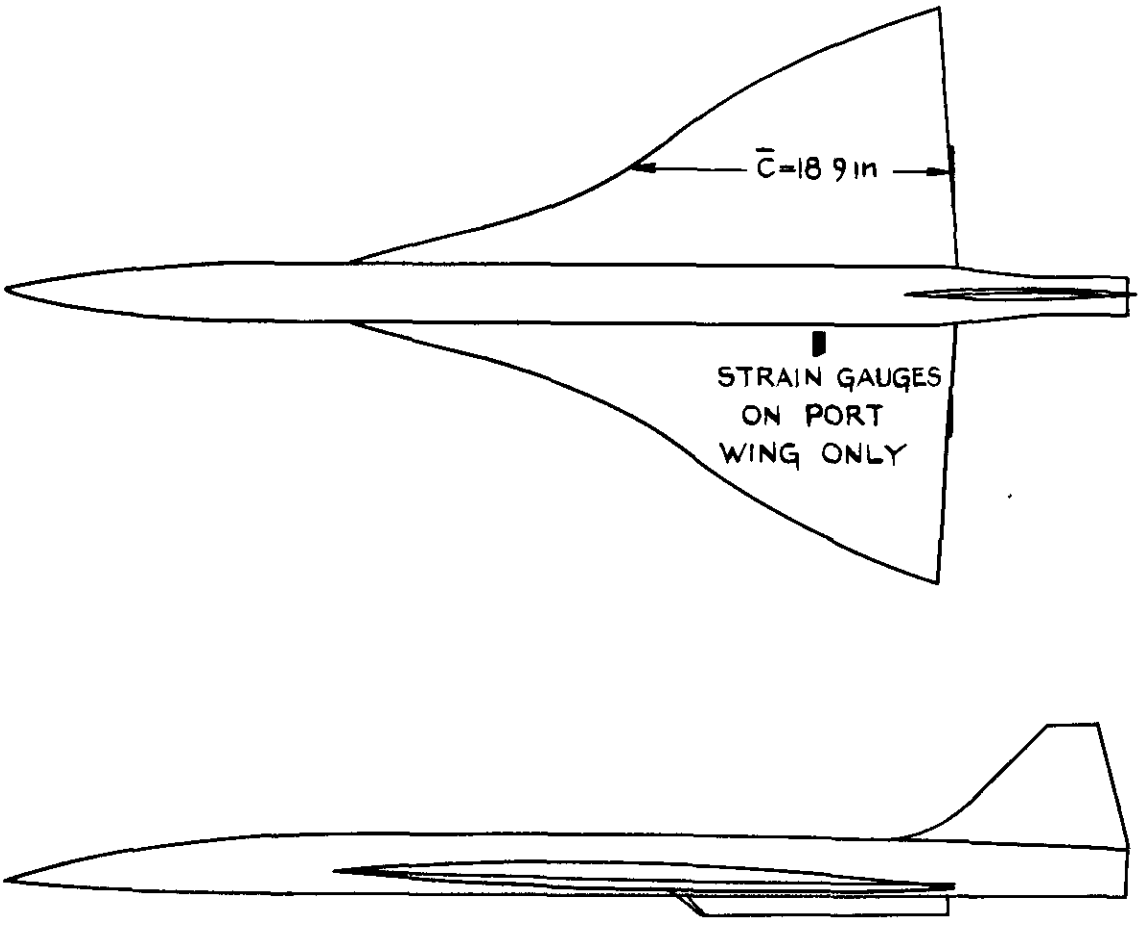

FIG. 3 G.A OF MODEL 2

(FULL SCALE FREQUENCIES IN BRACKETS)

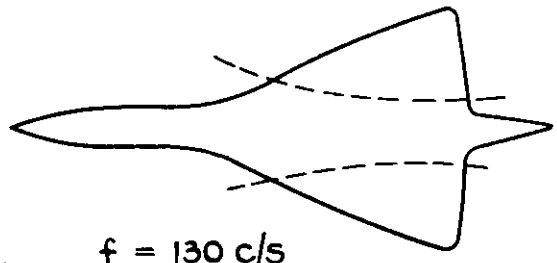

1ST DISTORTION MODE

f = 130 c/s

$g/2$ = 0·0042

(4·3 c/s)

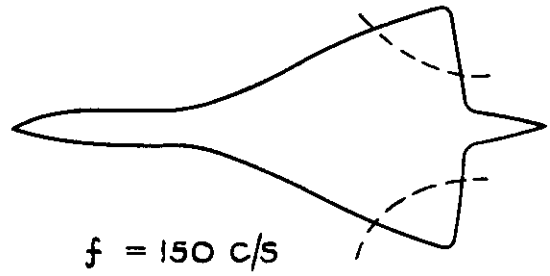

2nd DISTORTION MODE

f = 150 c/s

$g/2$ = 0·00082

(5·0 c/s)

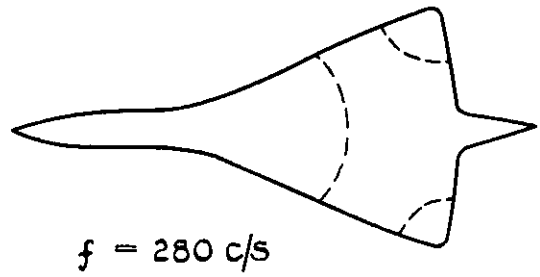

3rd DISTORTION MODE

f = 280 c/s

$g/2$ = 0·00048

(9·3 c/s)

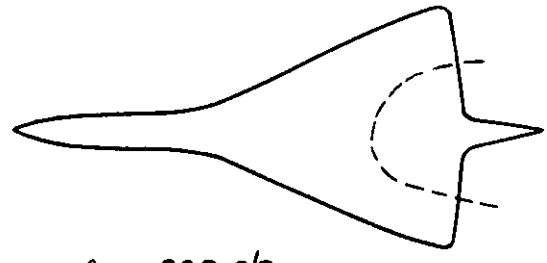

4th DISTORTION MODE

f = 320 c/s

$g/2$ = 0·0020

(10·7 c/s)

FIG.4 MODEL 2 DISTORTION MODES

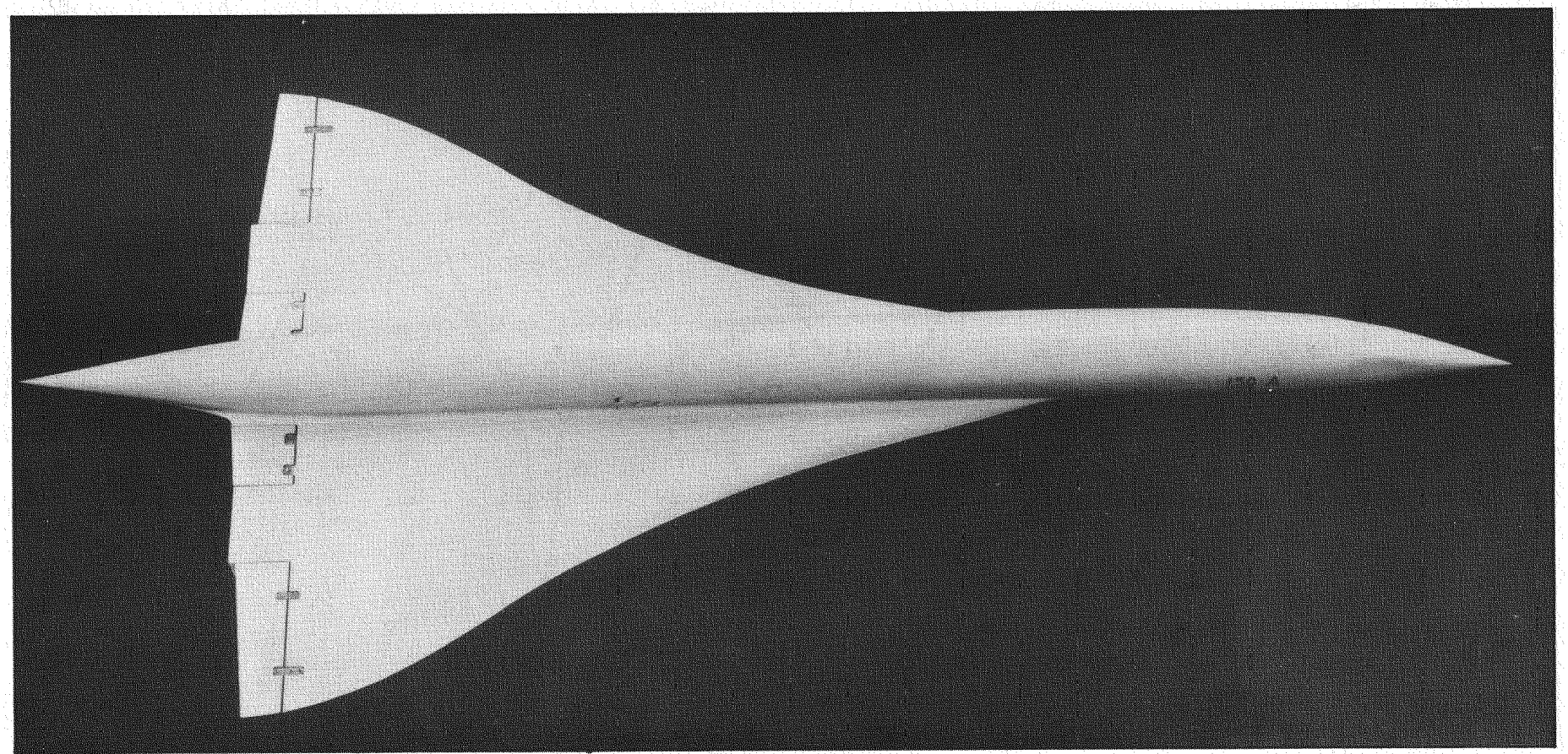

Fig.5. Model 3.

(FULL SCALE FREQUENCIES IN BRACKETS)

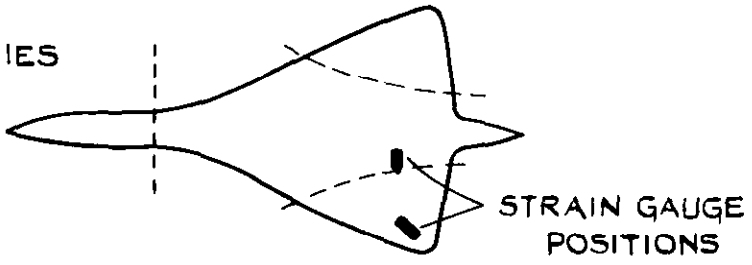

1st DISTORTION MODE

f = 127·5 c/s (2·3 c/s)

$g/2$ = 0·011

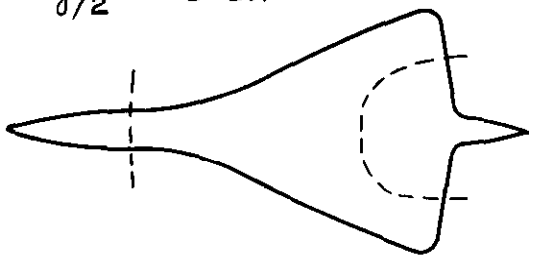

2nd DISTORTION MODE

f = 155 c/s (2·8 c/s)

$g/2$ = 0·017

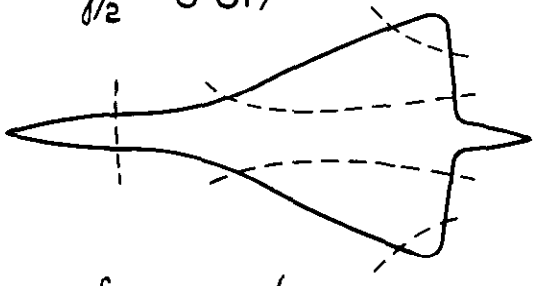

3rd DISTORTION MODE

f = 273 c/s (5·0 c/s)

$g/2$ = 0 0055

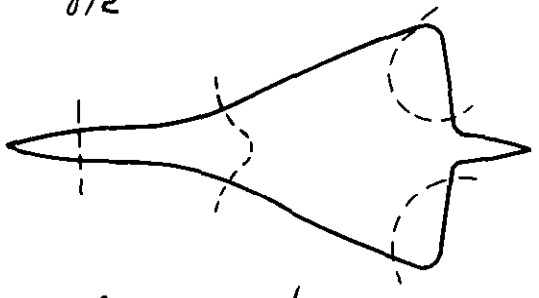

4th DISTORTION MODE

f = 300 c/s (5·5 c/s)

$g/2$ = 0·005

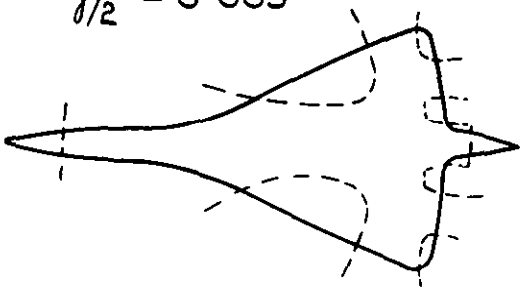

7th DISTORTION MODE

f = 535 c/s (9·7 c/s)

$g/2$ = 0·013

FIG.6 (a) SYMMETRIC MODES

FIG.6 MODEL 3 DISTORTION MODES

(FULL SCALE FREQUENCIES IN BRACKETS)

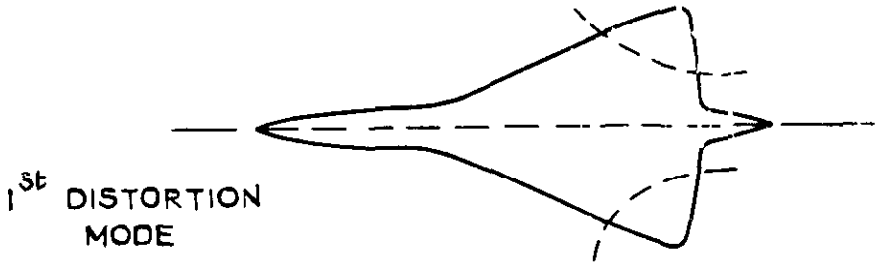

1st DISTORTION MODE

f = 153 c/s (2 8 c/s)

$g/2$ = 0 006

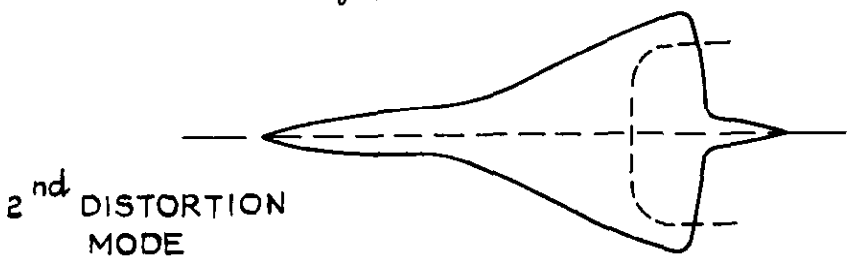

2nd DISTORTION MODE

f = 178 c/s (3·2 c/s)

$g/2$ = 0·012

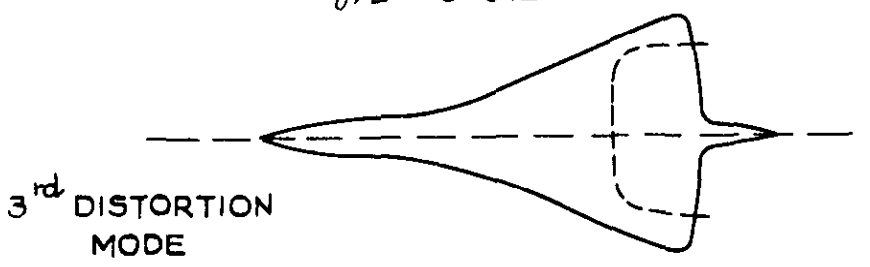

3rd DISTORTION MODE

f = 254 c/s (4·6 c/s)

$g/2$ = 0·006

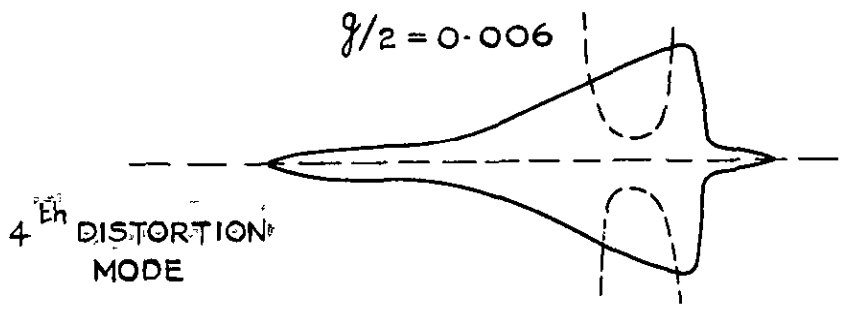

4th DISTORTION MODE

f = 342 c/s (6·2 c/s)

$g/2$ = 0·006

FIG. 6 (b) ANTISYMMETRIC MODES

FIG. 6 (CONCLD.) MODEL 3 DISTORTION MODES

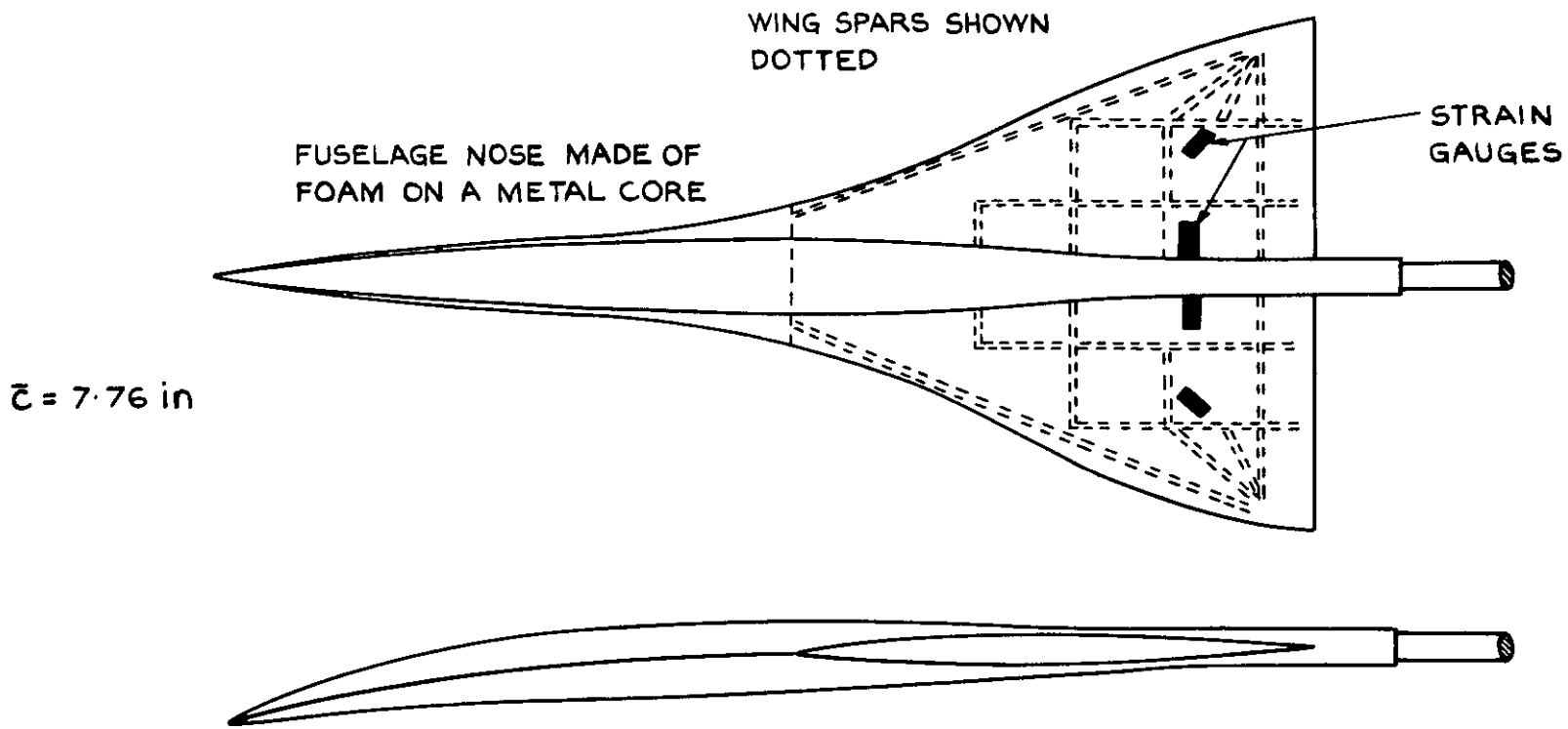

FIG. 7 G.A. OF MODEL 4

(FULL SCALE FREQUENCIES IN BRACKETS)

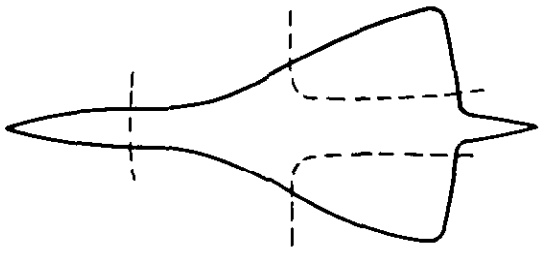

1st DISTORTION MODE

f = 263 c/s (3·5 c/s)

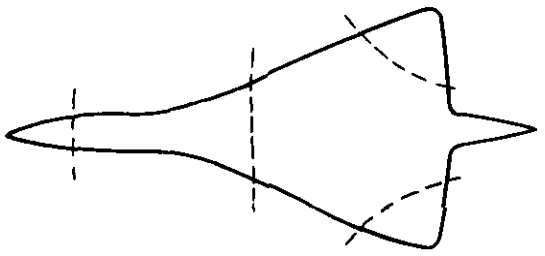

2nd DISTORTION MODE

f = 380 c/s (5·1 c/s)

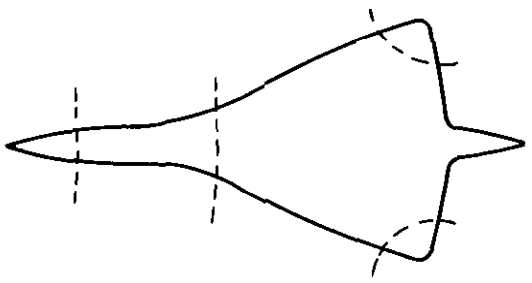

3rd DISTORTION MODE

f = 434 c/s (5·8 c/s)

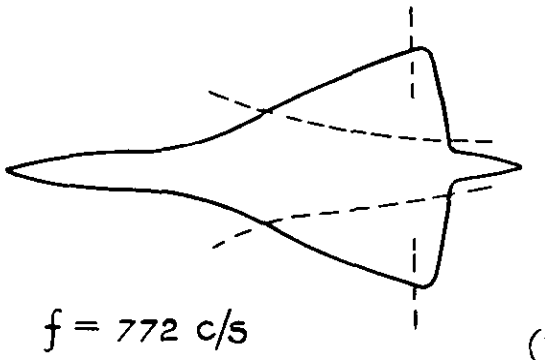

4th DISTORTION MODE

f = 772 c/s (10·3 c/s)

FIG. 8 MODEL 4 DISTORTION MODES (APPROX.)

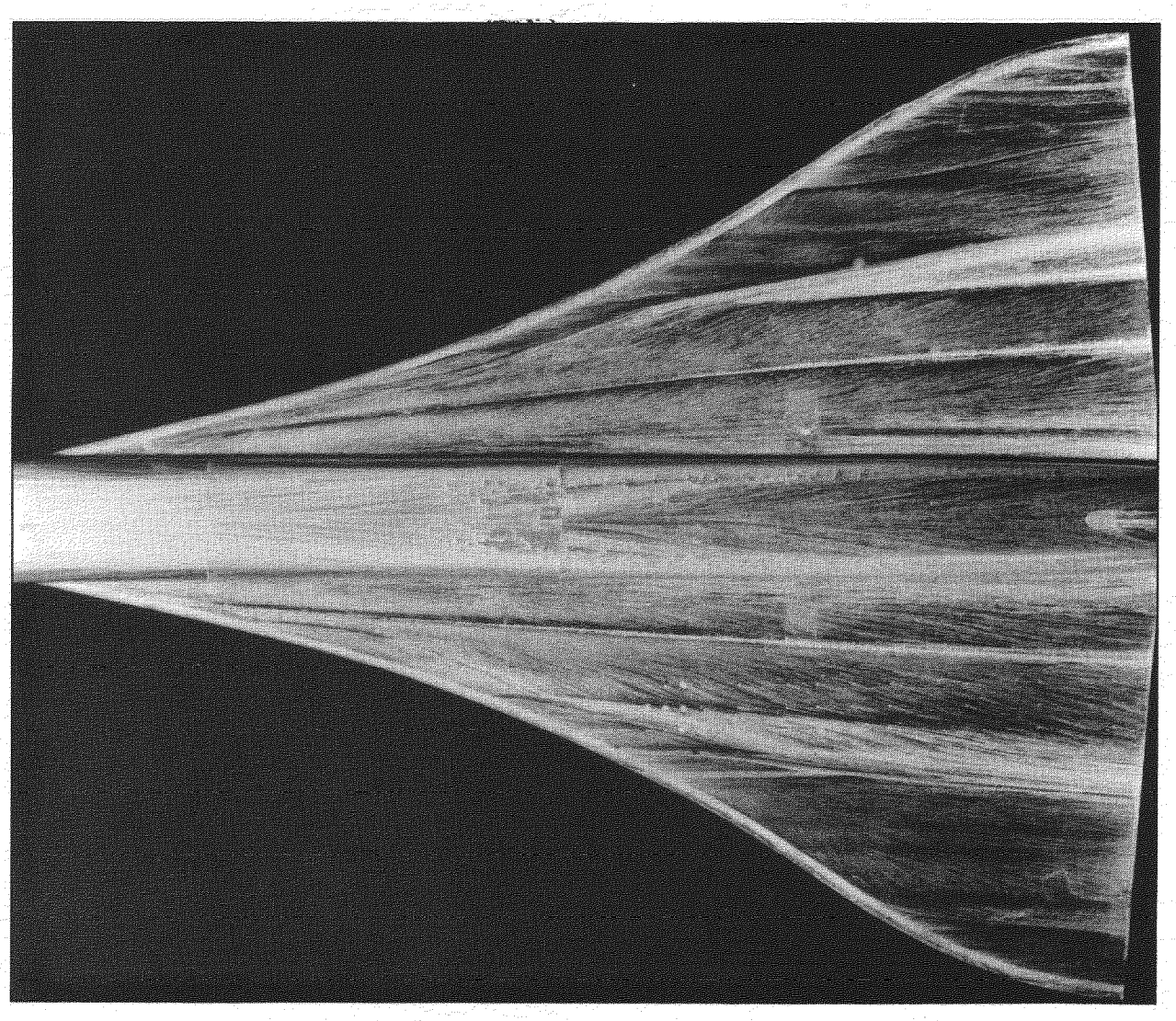

(a)α=6°

Fig.9. Model 1-oil flow photographs near mild buffet onset M=0.40.

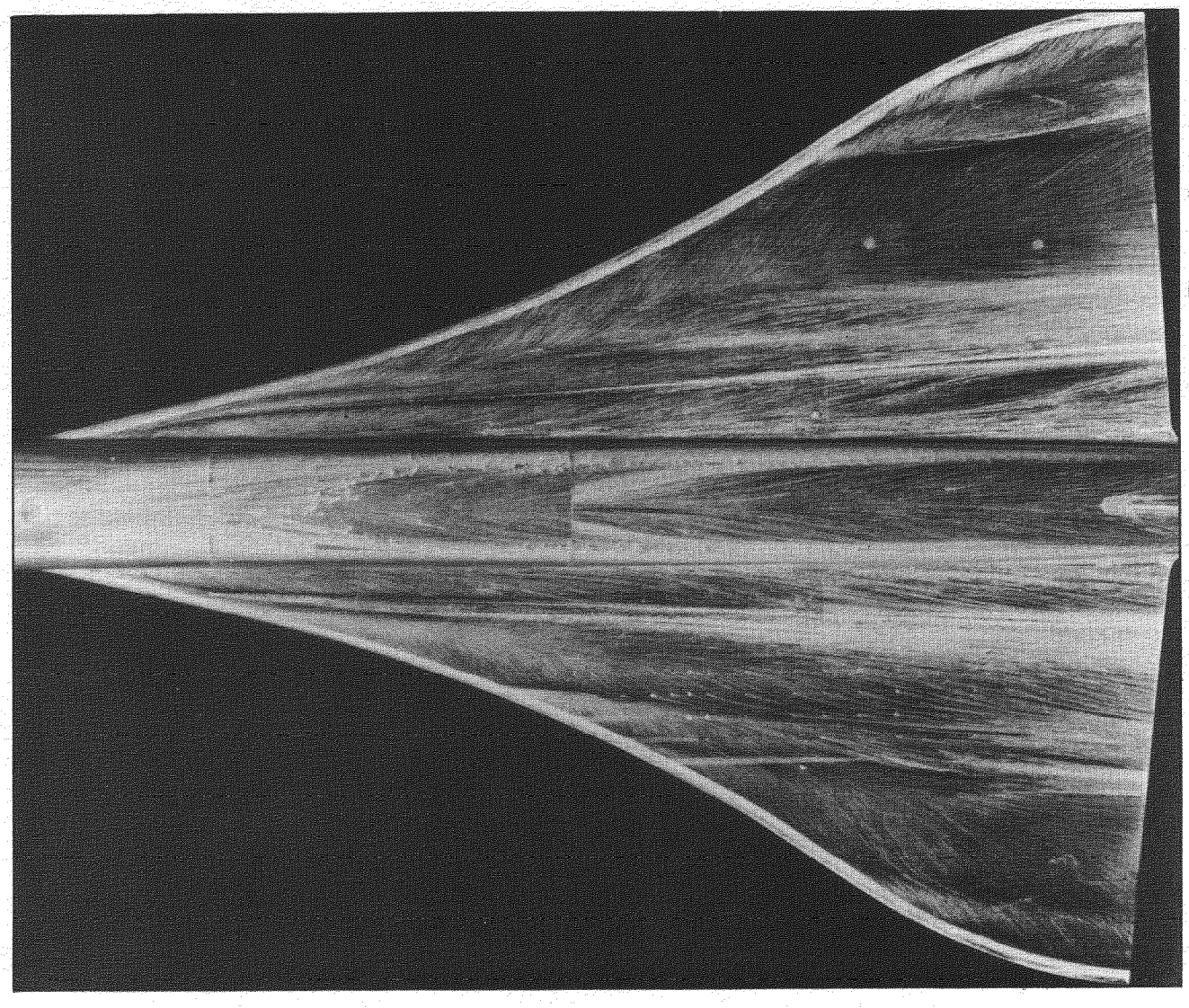

(b)$\alpha=7^{\circ}$

Fig.9. (cont'd).

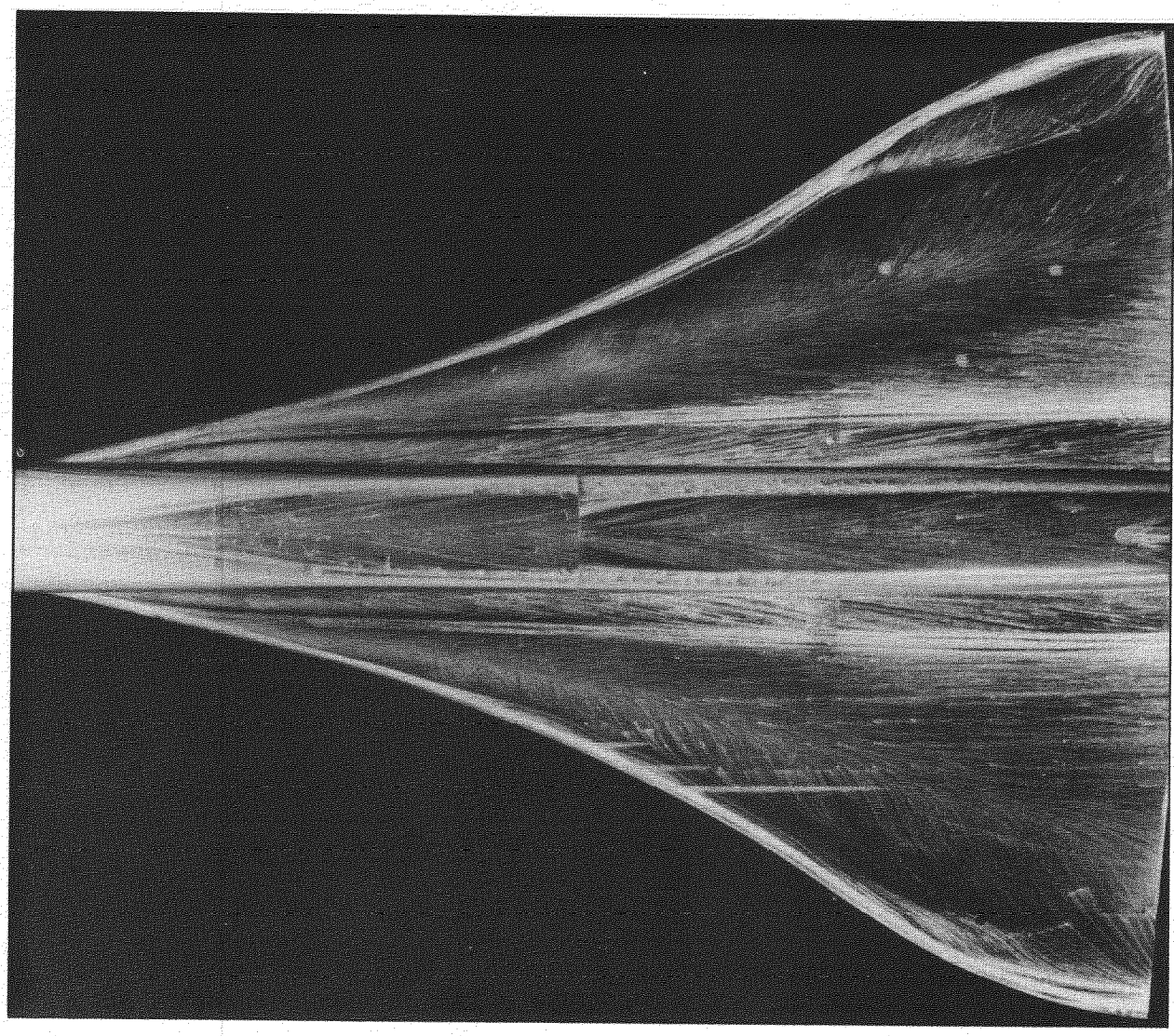

(c) $\alpha = 8°$

Fig.9. (concl'd).

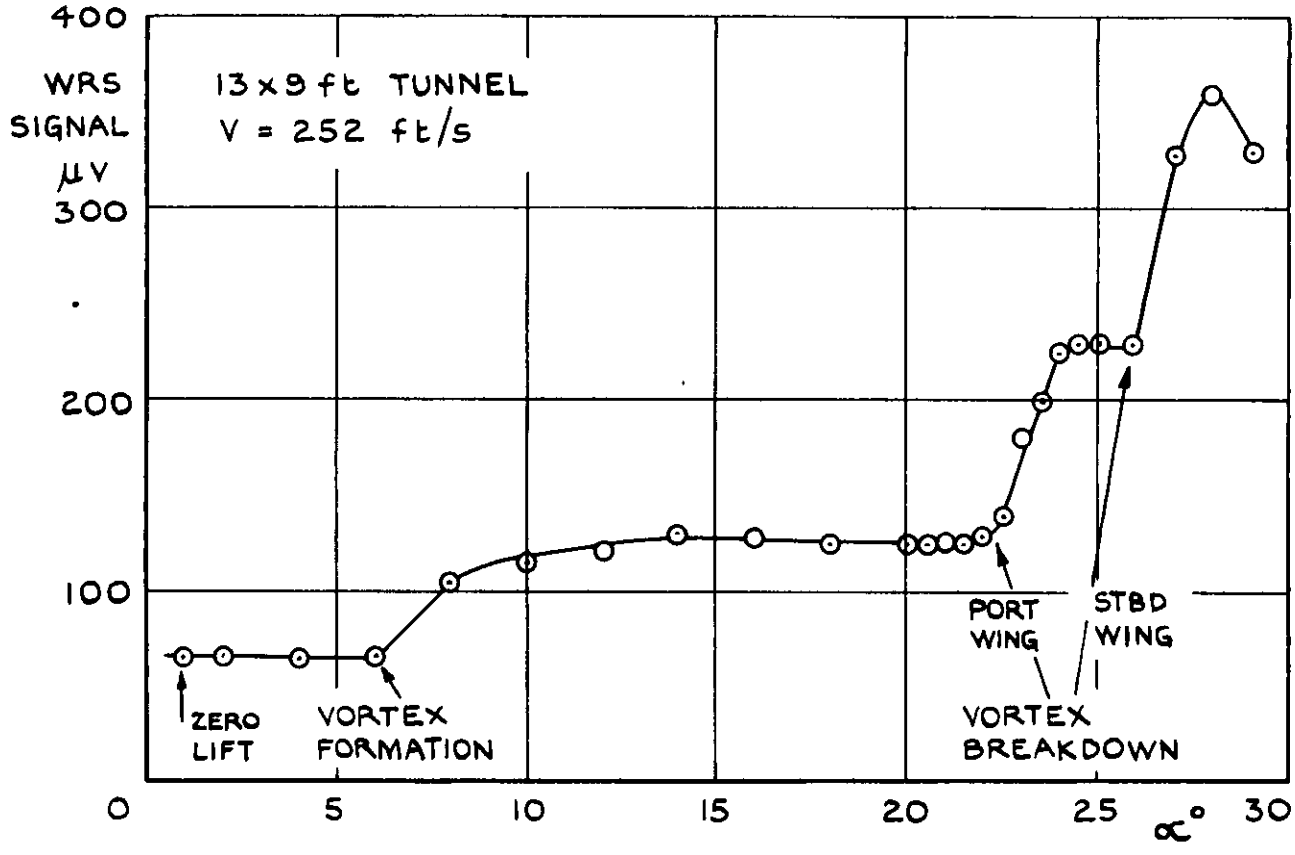

FIG. 10 MODEL 1 VARIATION OF TOTAL WING-ROOT STRAIN SIGNAL WITH INCIDENCE

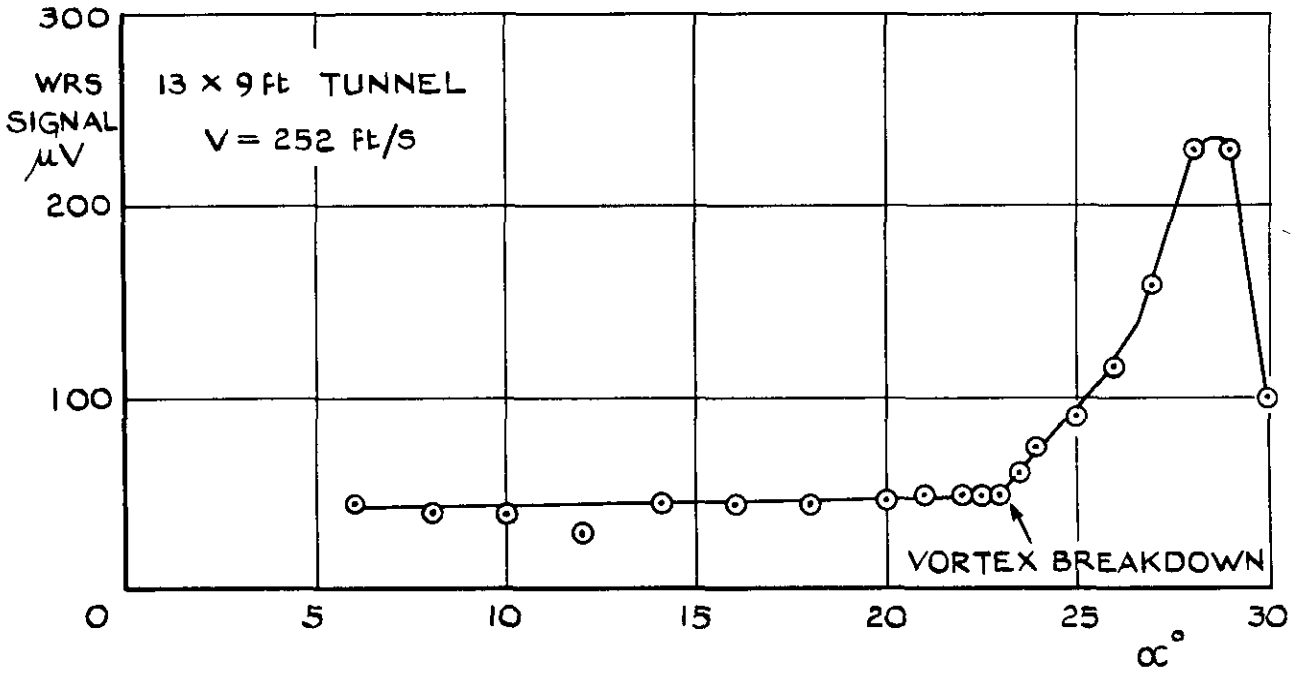

FIG.11(a) f = 300 c/s

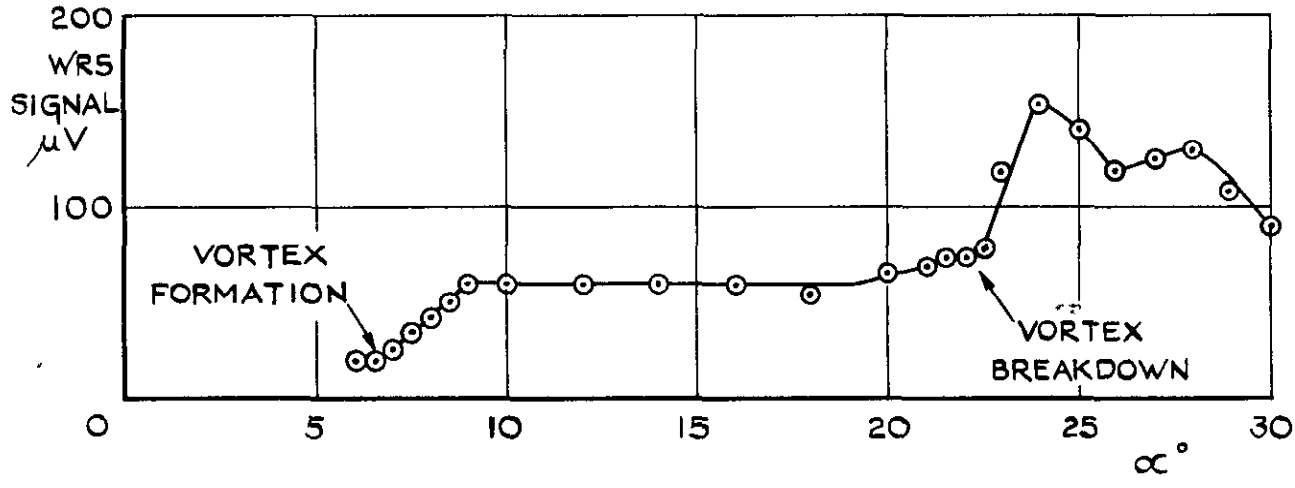

FIG.11 (b) f = 700 c/s

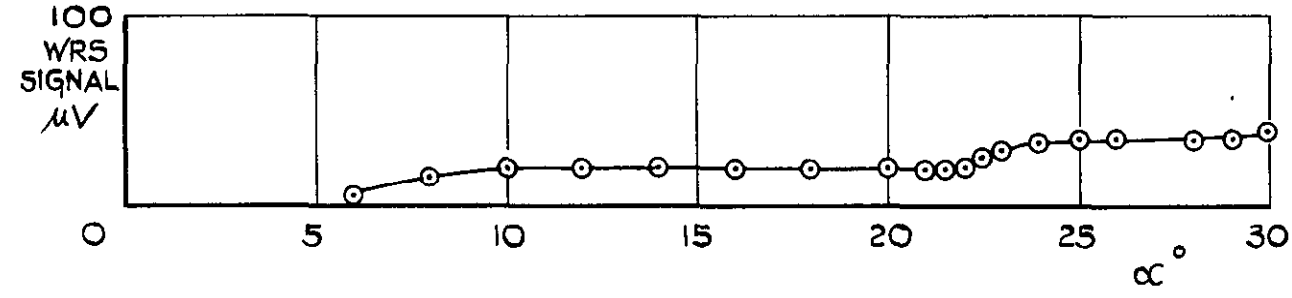

FIG.11(c) f = 1330 c/s

FIG. 11 MODEL I VARIATION OF TUNED WING–ROOT STRAIN SIGNAL WITH INCIDENCE

13 x 9 ft TUNNEL

V = 252 ft/s

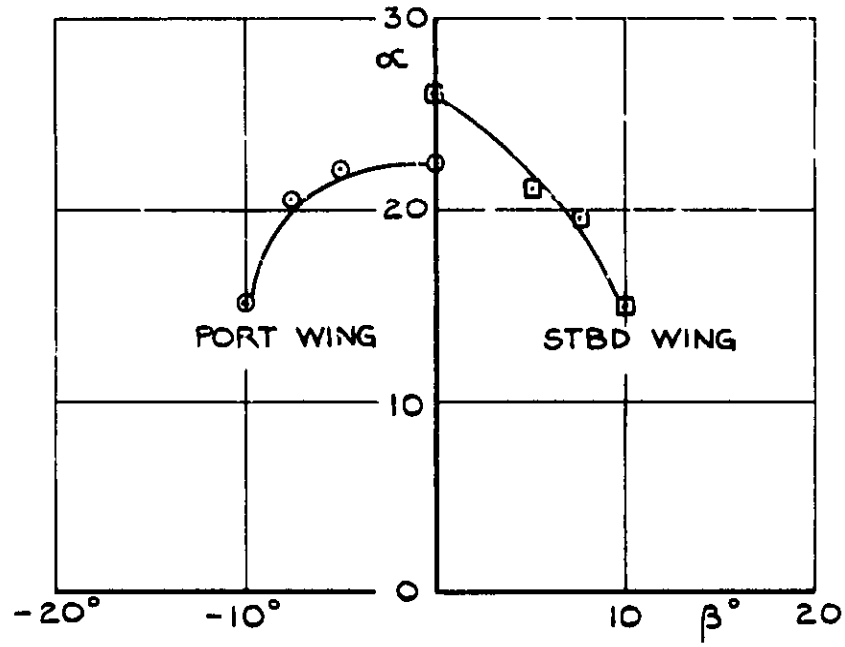

FIG.12 MODEL I EFFECT OF SIDESLIP ON INCIDENCE FOR VORTEX BREAKDOWN

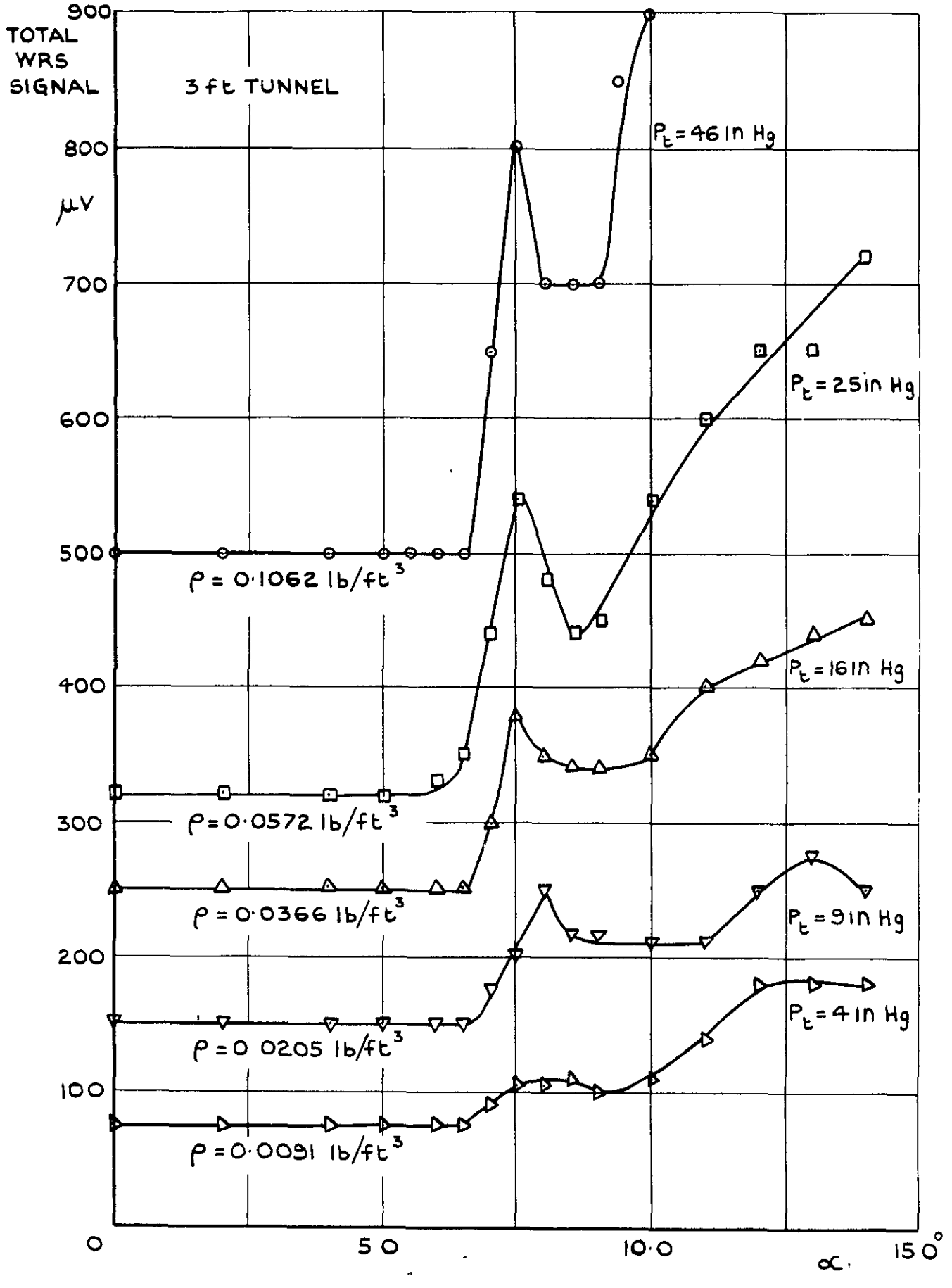

FIG.13 MODEL I VARIATION OF TOTAL WING-ROOT STRAIN SIGNAL WITH INCIDENCE AND DENSITY M = 0·50

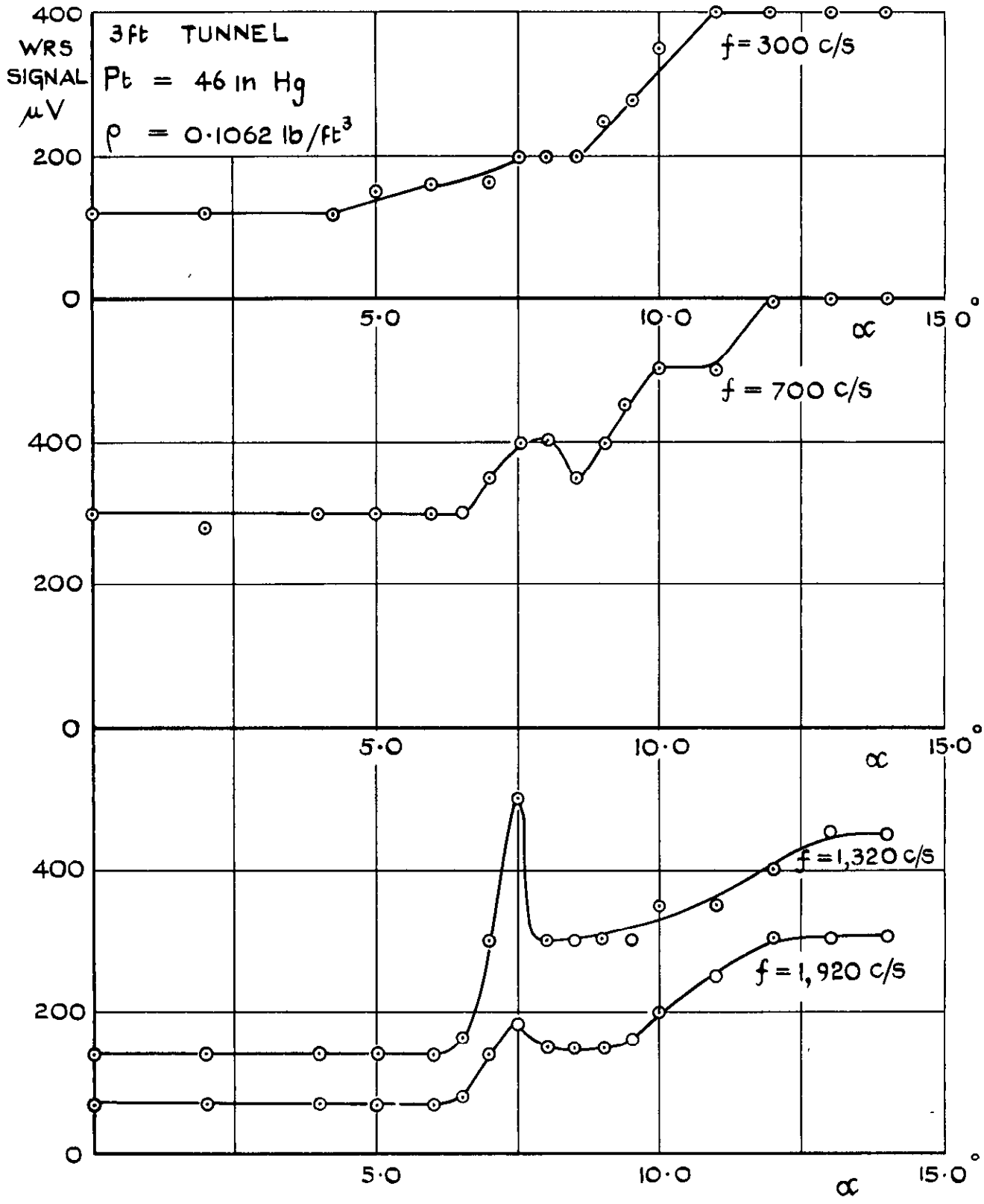

FIG. 14 MODEL I VARIATION OF TUNED WING-ROOT STRAIN SIGNAL WITH INCIDENCE M = 0·50

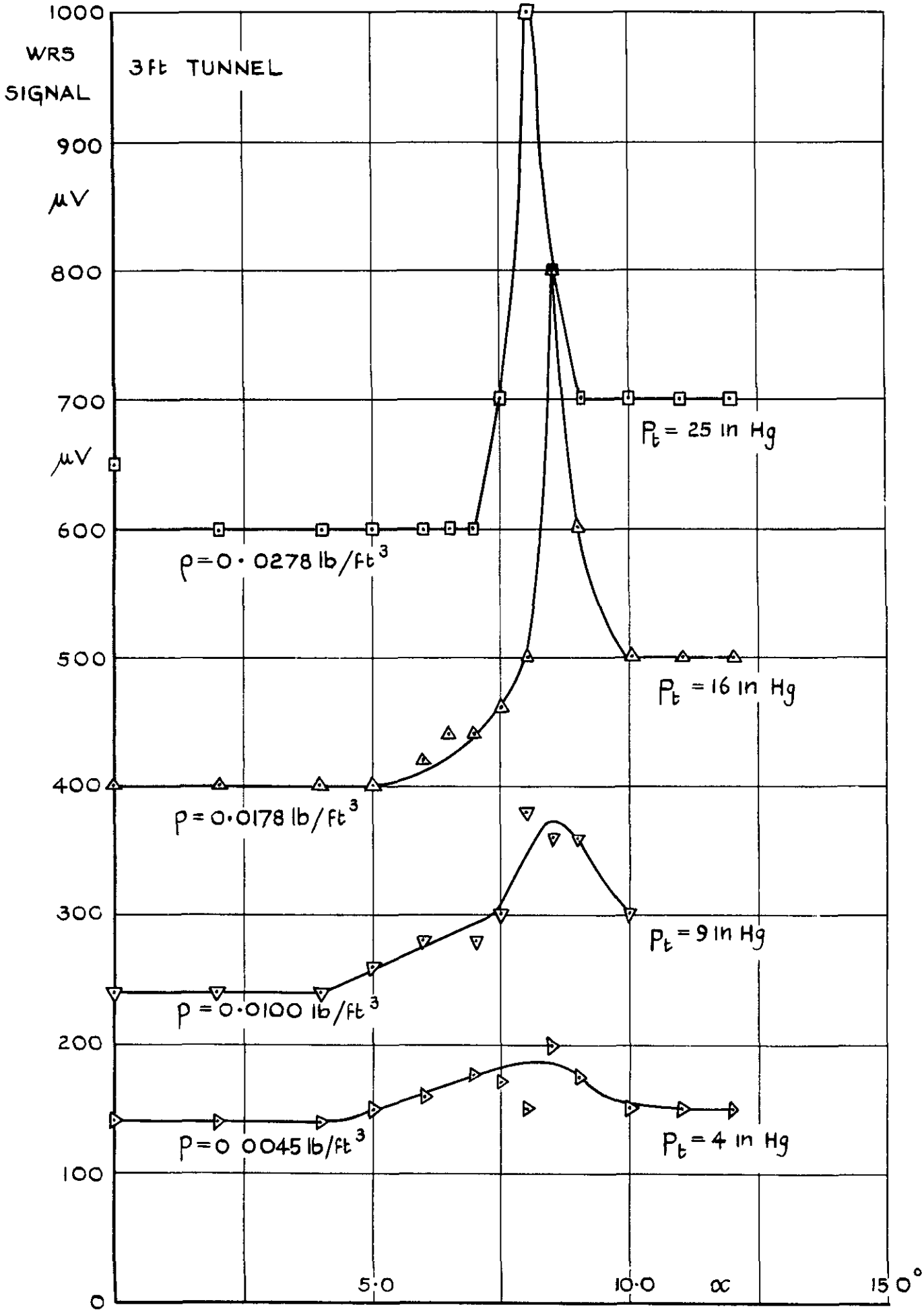

FIG.15 MODEL 1 VARIATION OF TOTAL WING-ROOT STRAIN SIGNAL WITH INCIDENCE AND DENSITY M=1·4

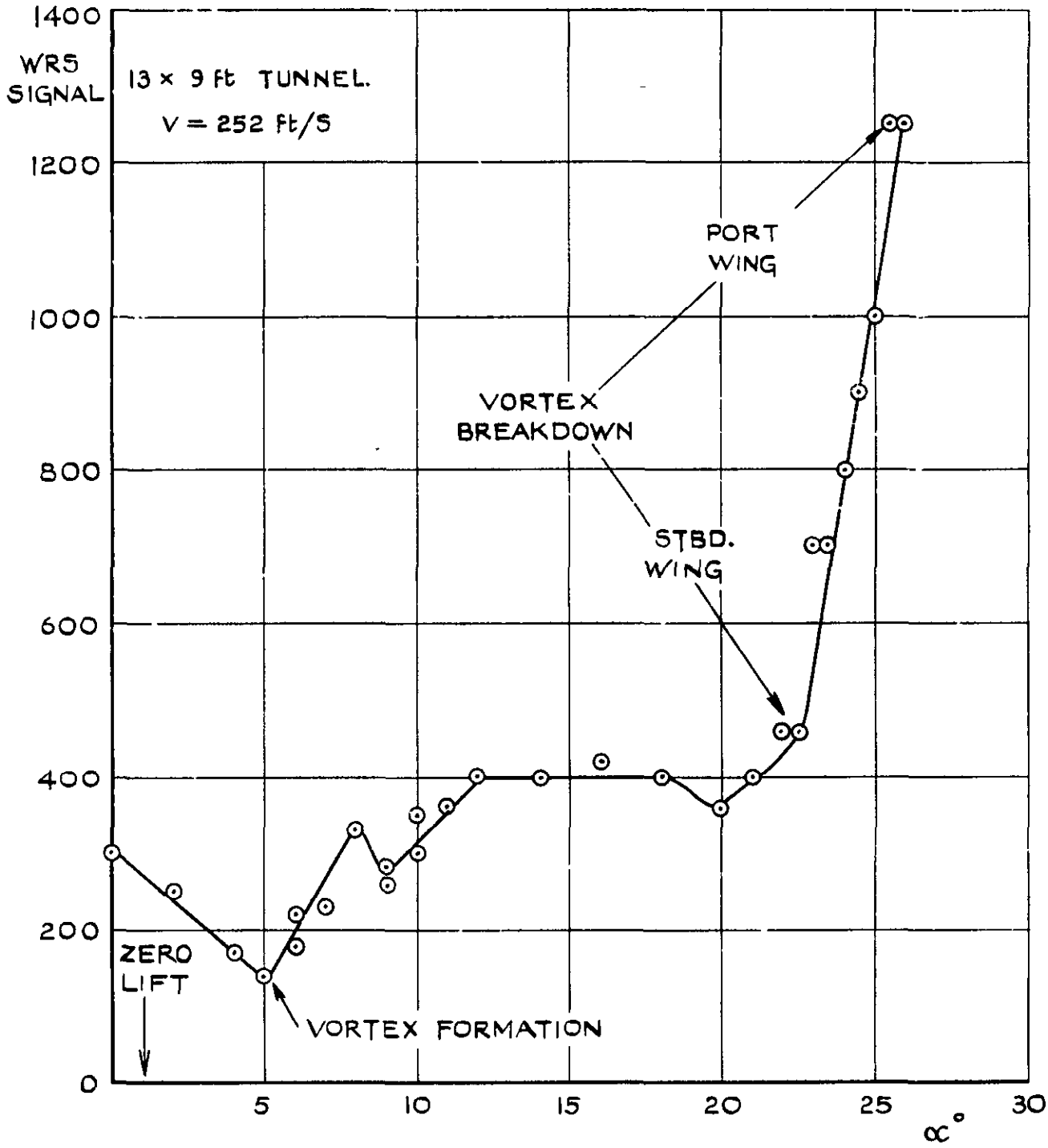

FIG. 16 MODEL 2 VARIATION OF TOTAL WING-ROOT STRAIN SIGNAL WITH INCIDENCE

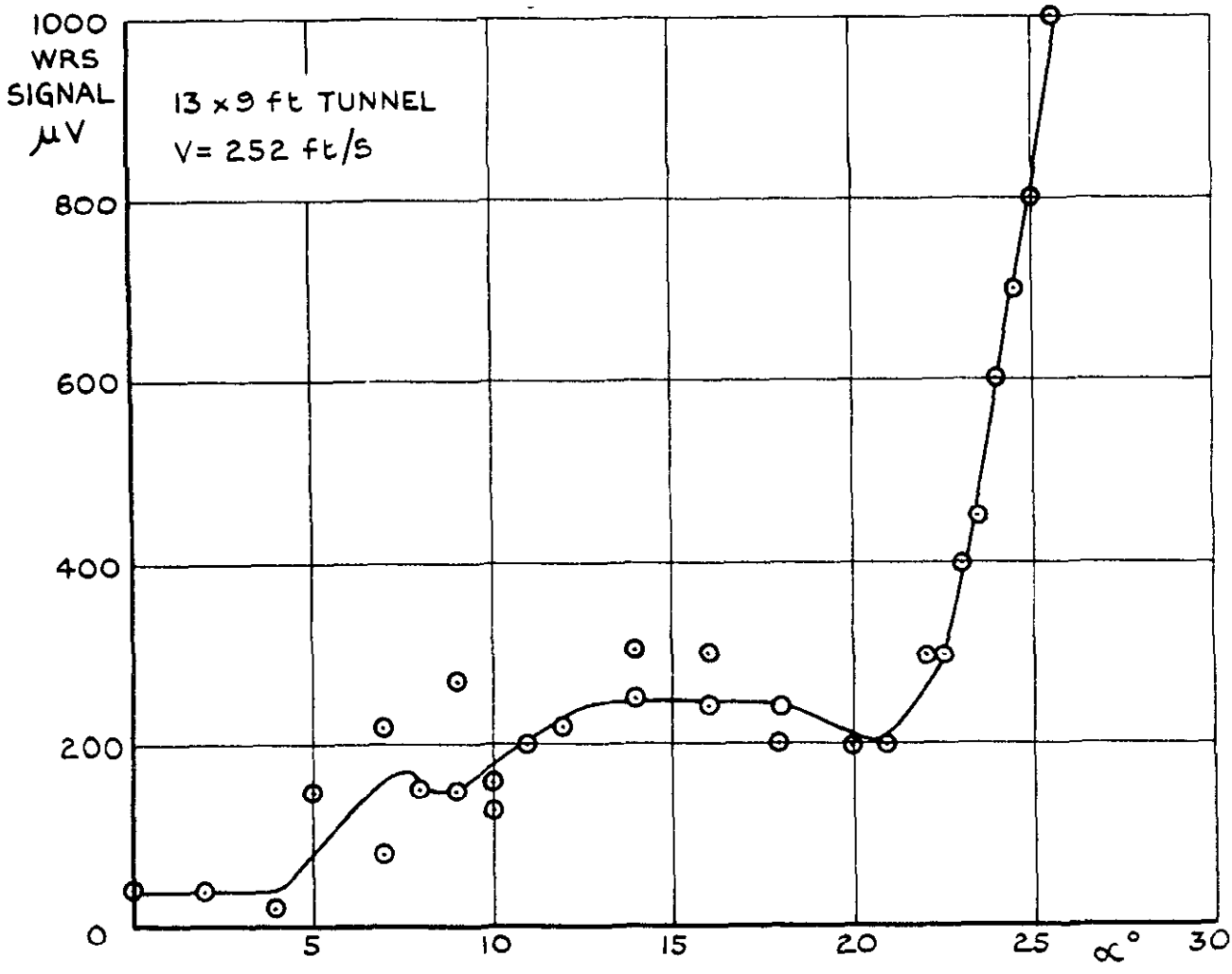

FIG 17 (a) f = 128 C/S

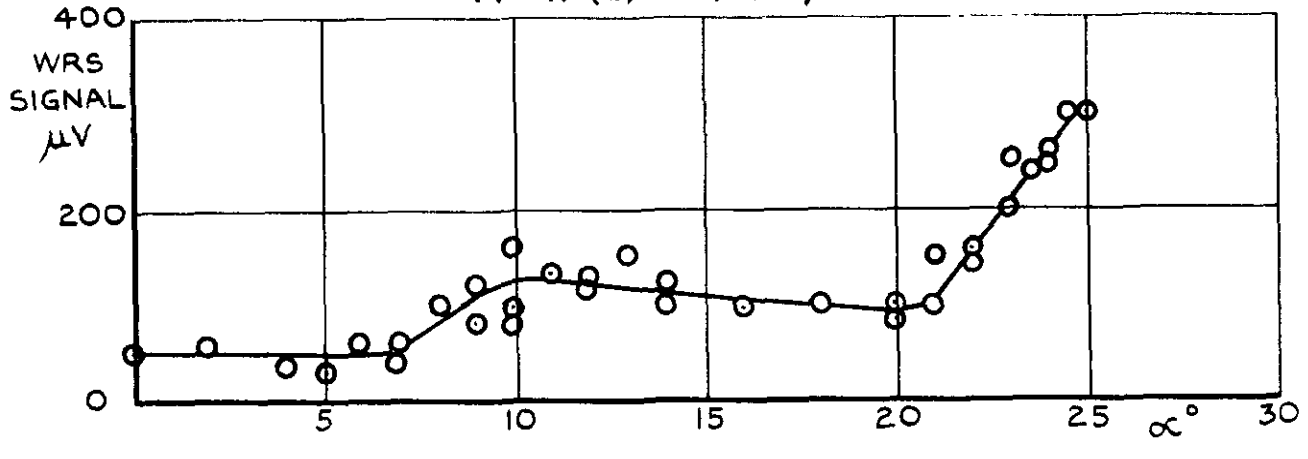

FIG. 17 (b) f = 150 C/S

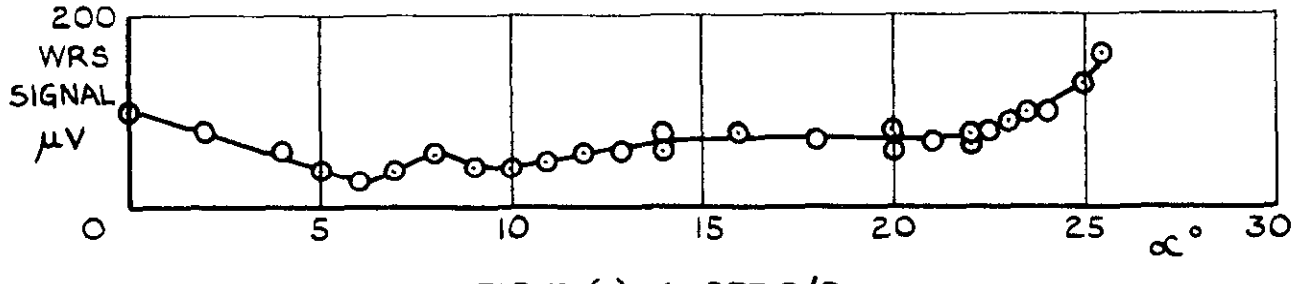

FIG. 17 (c) f = 277 C/S

FIG. 17 MODEL 2 VARIATION OF TUNED WING-ROOT STRAIN SIGNAL WITH INCIDENCE

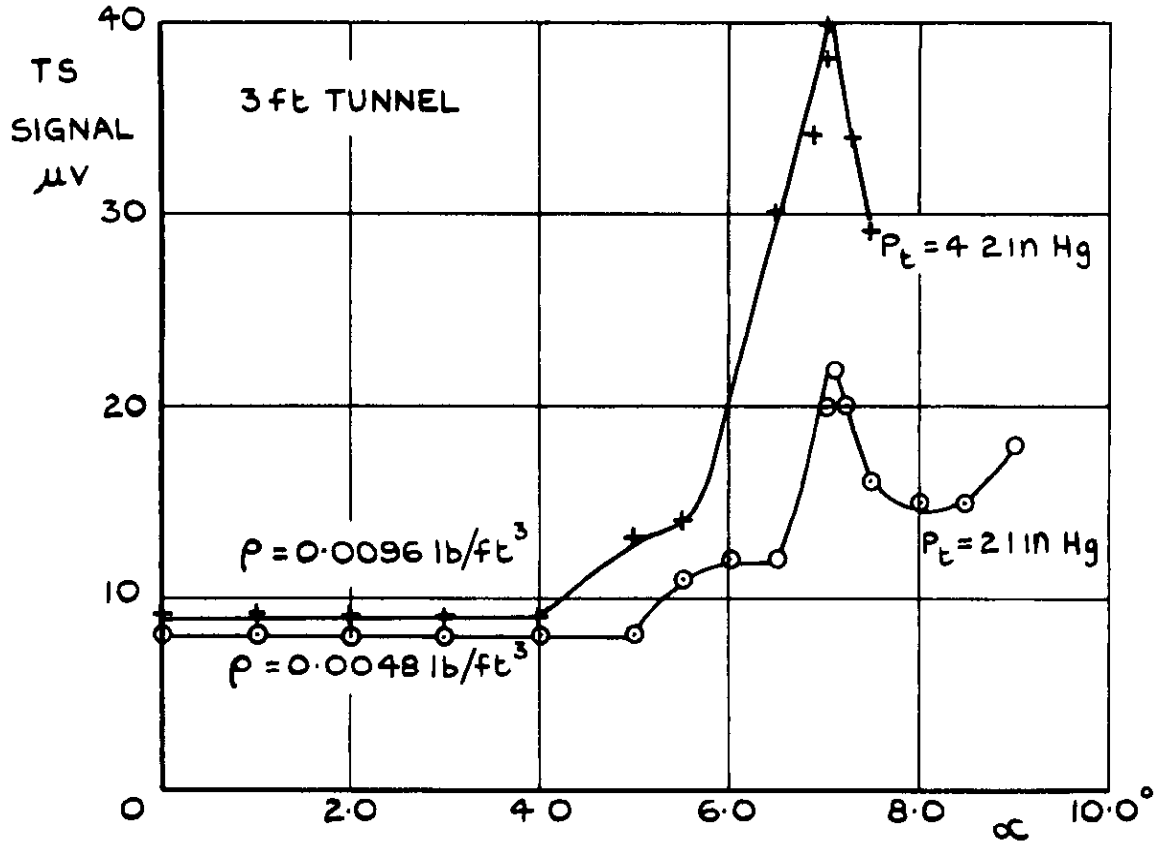

FIG.18 (a) UNCORRECTED FOR "PICK UP" AND UNSTEADINESS

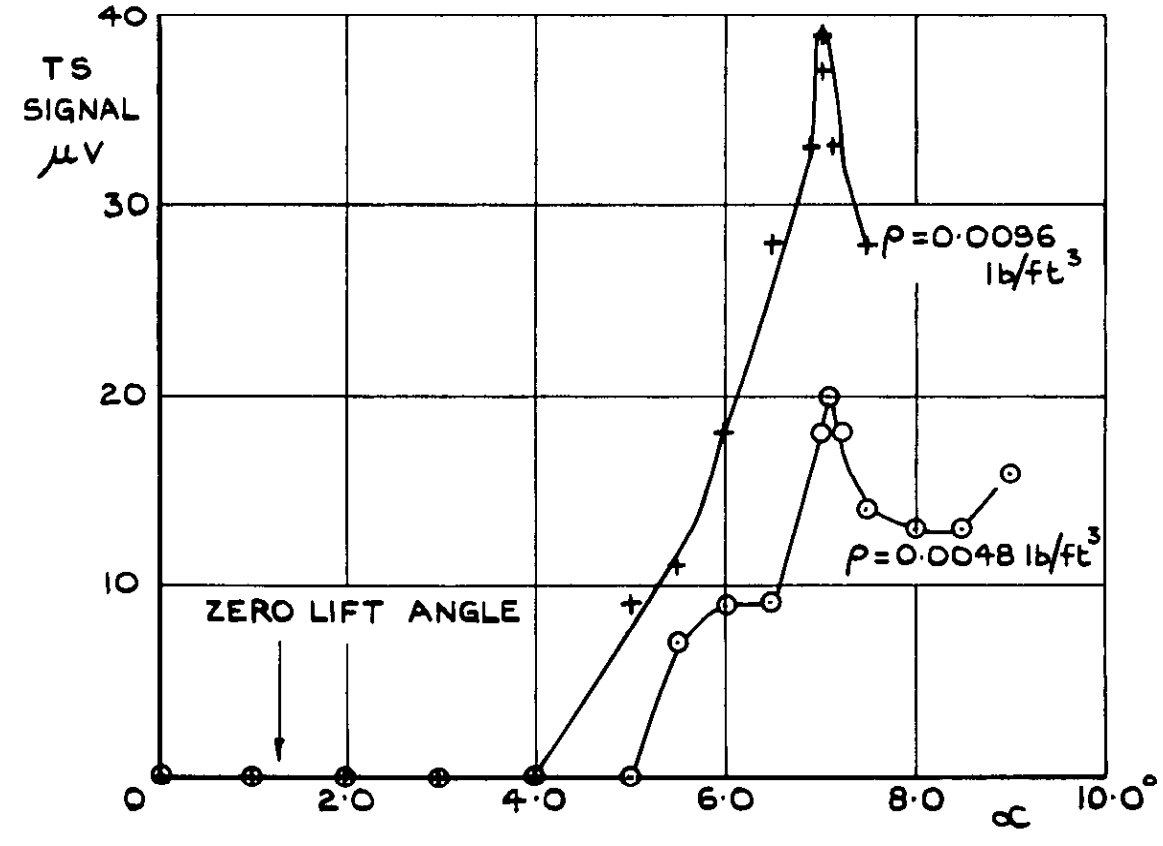

FIG.18 (b) CORRECTED FOR "PICK UP" AND UNSTEADINESS

FIG.18 MODEL 3 VARIATION OF TOTAL TIP-STRAIN SIGNAL WITH INCIDENCE AND DENSITY M=0·50

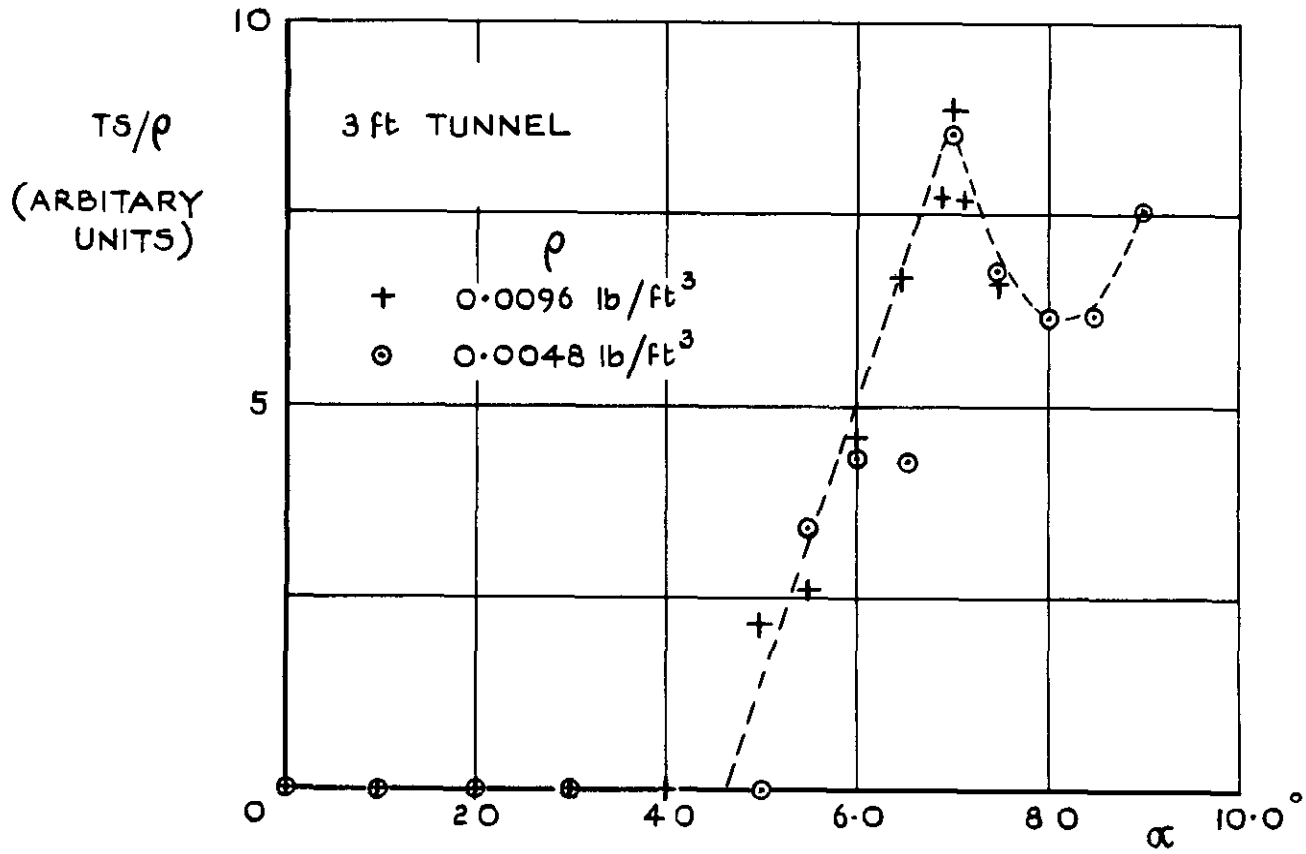

FIG.(a) T S SIGNAL/(DENSITY) v INCIDENCE

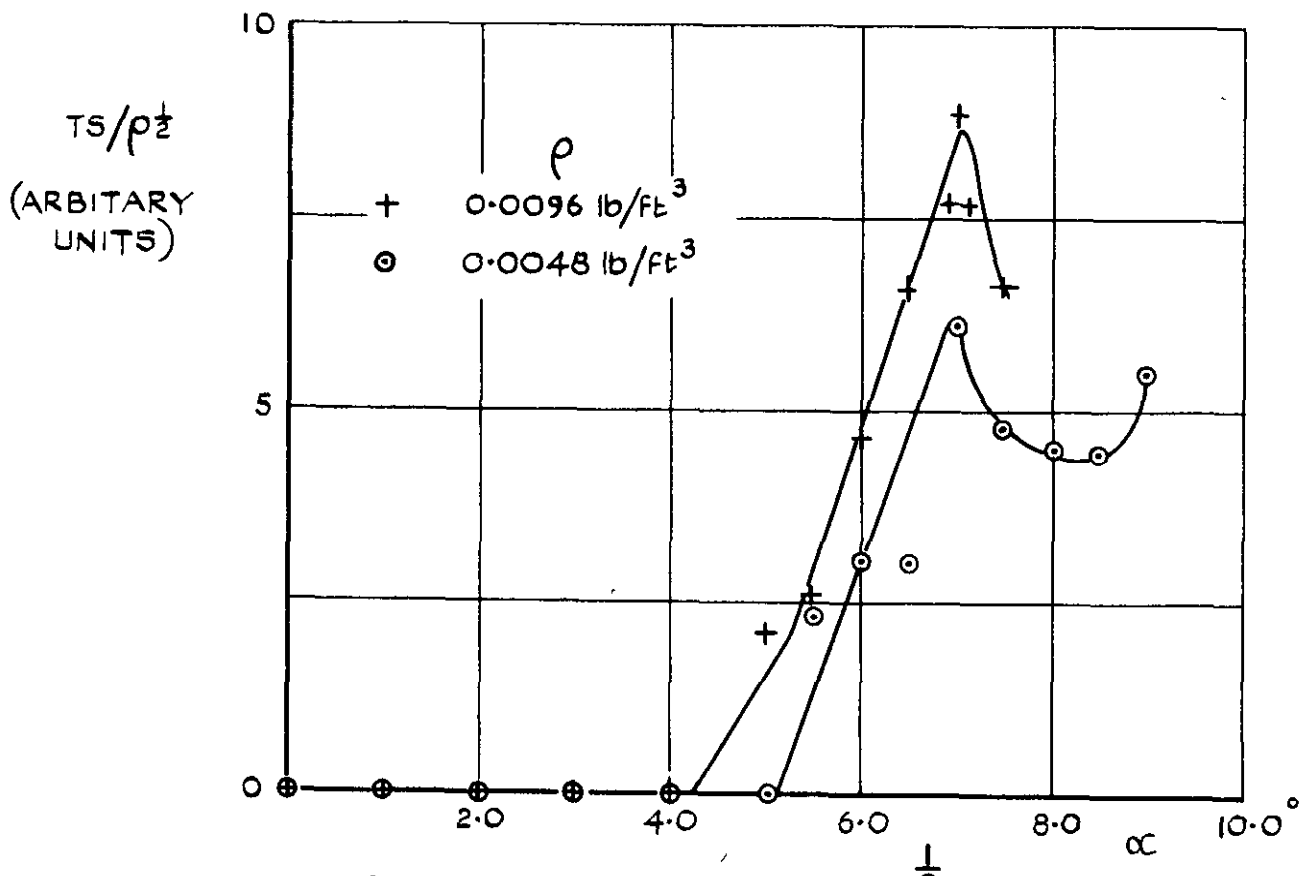

FIG.19 (b) T S SIGNAL / (DENSITY) $^{\frac{1}{2}}$ v INCIDENCE

FIG.19 MODEL 3 COMPARISON OF BUFFETING SCALING LAWS M=0·50

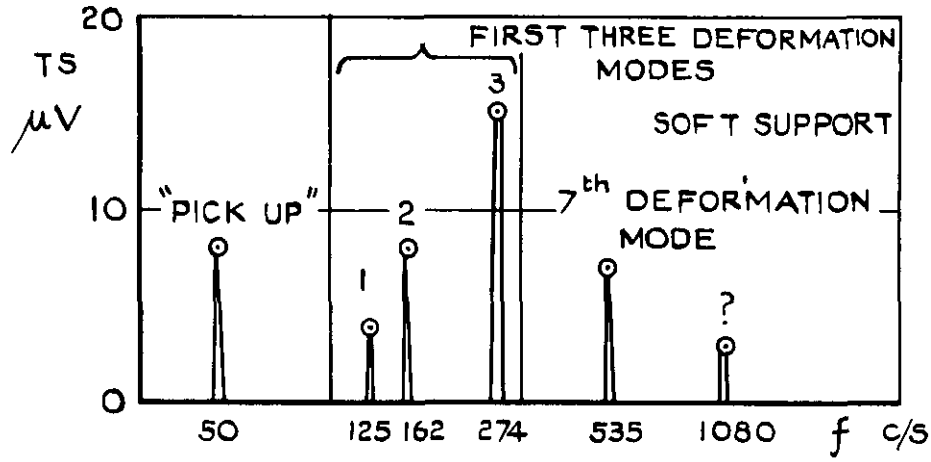

FIG.20 (a) TIP-STRAIN $\rho = 0.00478$ lb/ft^3 $\alpha = 7.10^\circ$

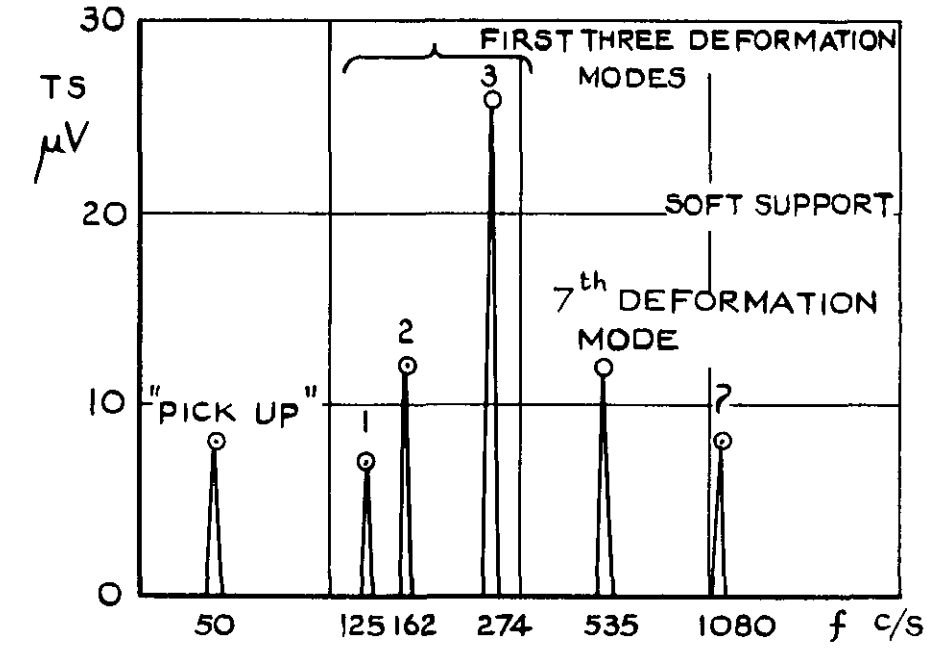

FIG. 20 (b) TIP-STRAIN $\rho = 0.00956$ lb/ft^3 $\alpha = 7.0^\circ$

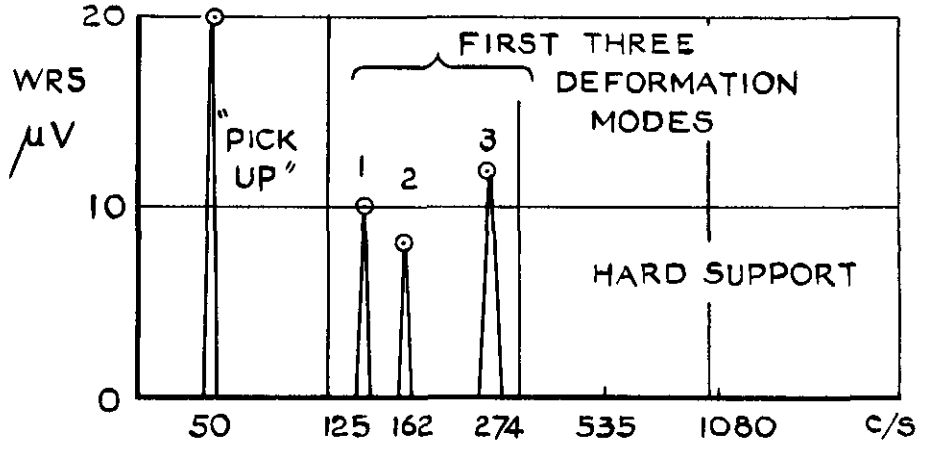

FIG. 20 (c) WING-ROOT STRAIN $\rho = 0.00956$ lb/ft^3 $\alpha = 9.0^\circ$

FIG.20 MODEL 3 SPECTRA OF STRAIN SIGNALS M=0.50

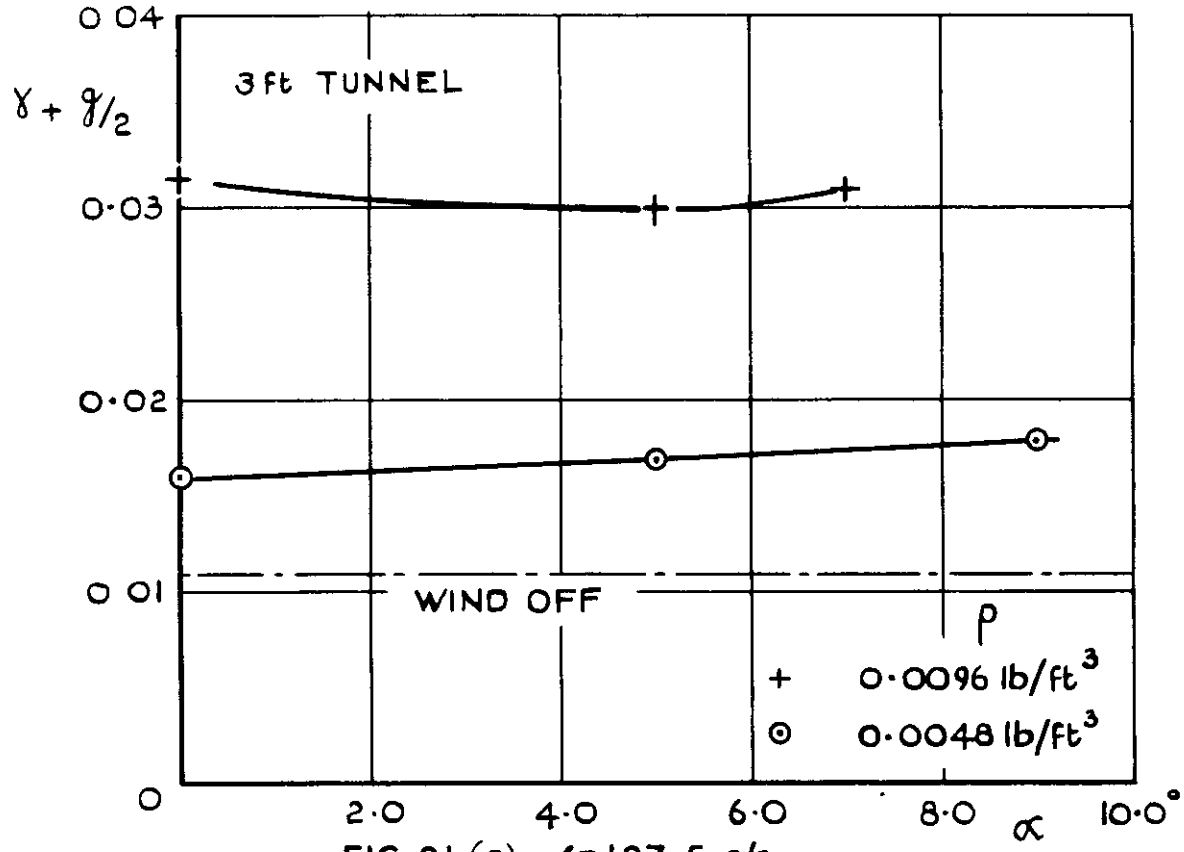

FIG. 21 (a) f=127·5 c/s

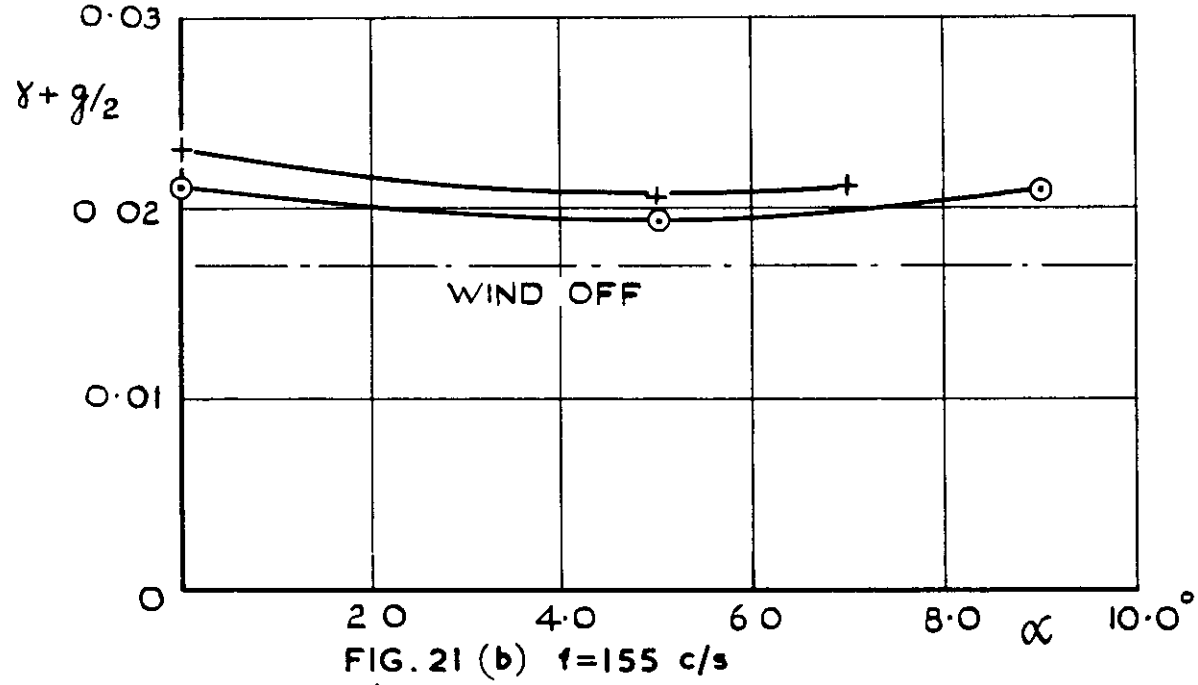

FIG. 21 (b) f=155 c/s

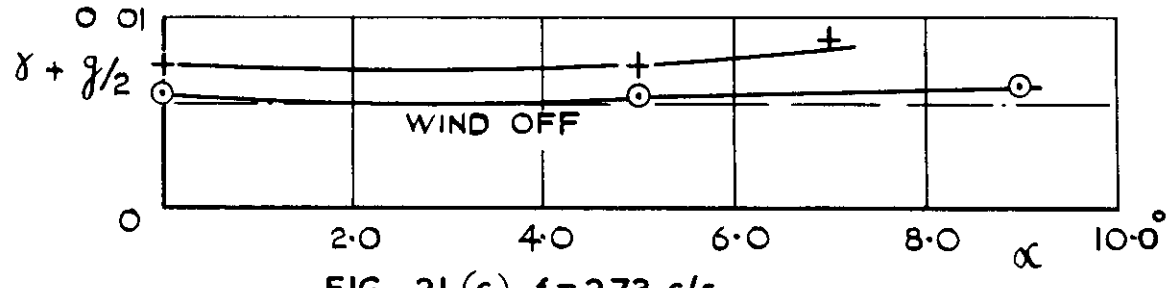

FIG. 21 (c) f=273 c/s

FIG. 21 MODEL 3 VARIATION OF TOTAL DAMPING COEFFIENTS FOR SYMMETRIC MODES WITH INCIDENCE AND DENSITY, M=0·50

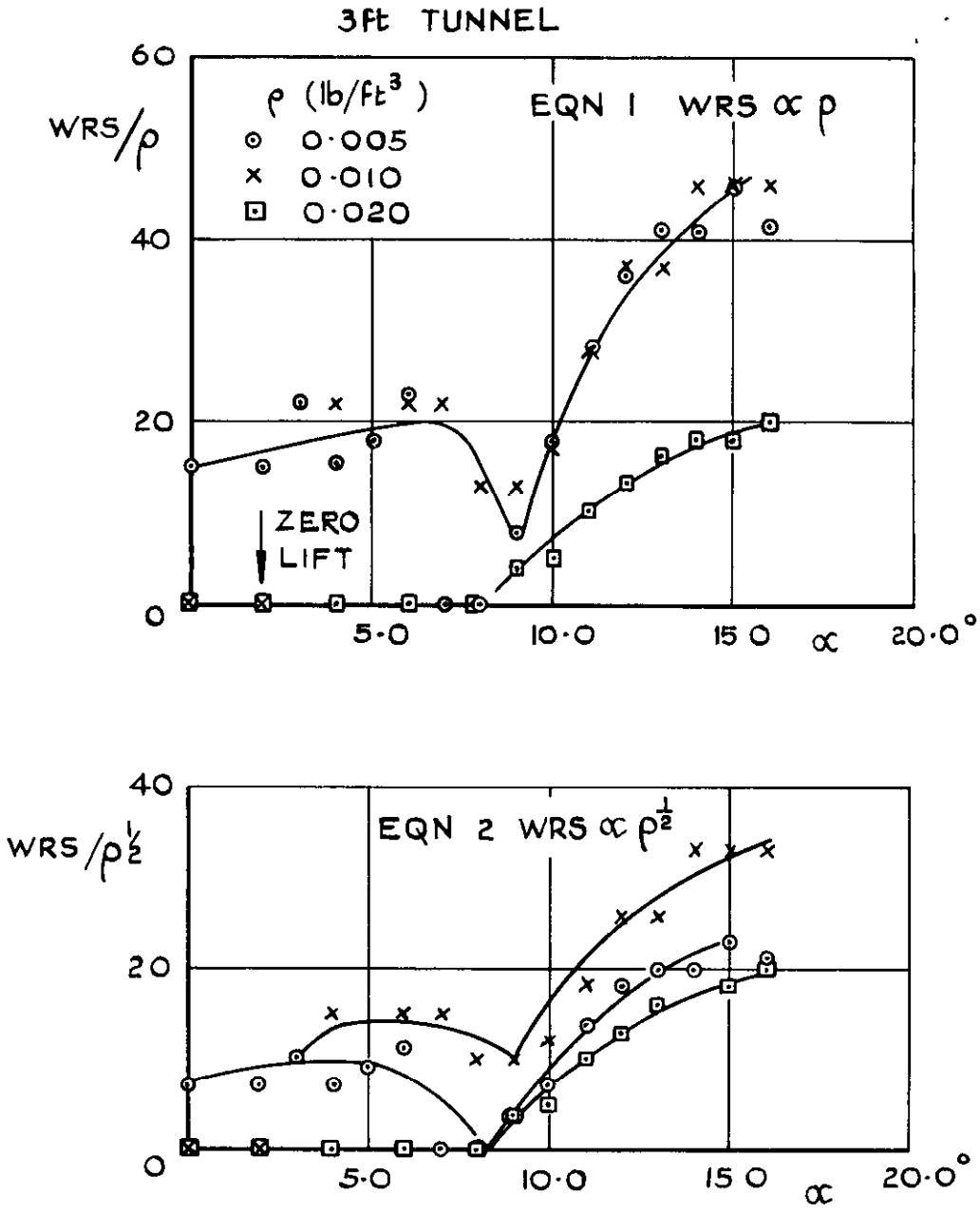

FIG. 22 (a) FUNDAMENTAL f= 263 c/s

FIG 22 MODEL 4 COMPARISON OF BUFFETING SCALING RELATIONSHIPS FOR DIFFERENT MODES M=0·40

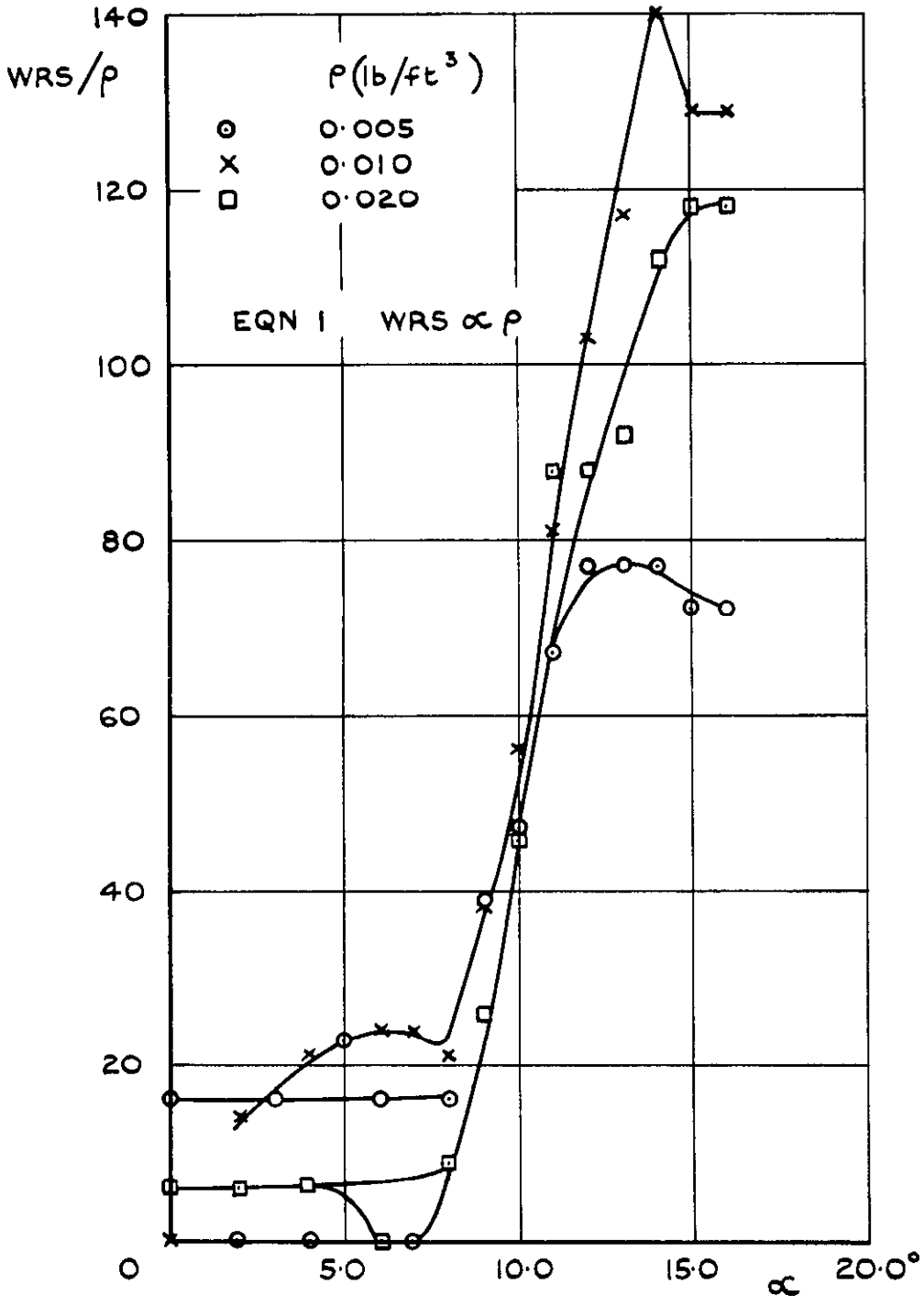

FIG 22 (b1) f = 380 C/S

FIG. 22 (CONT'D) MODEL 4 COMPARISON OF BUFFETING SCALING RELATIONSHIPS FOR DIFFERENT MODES M=0·40

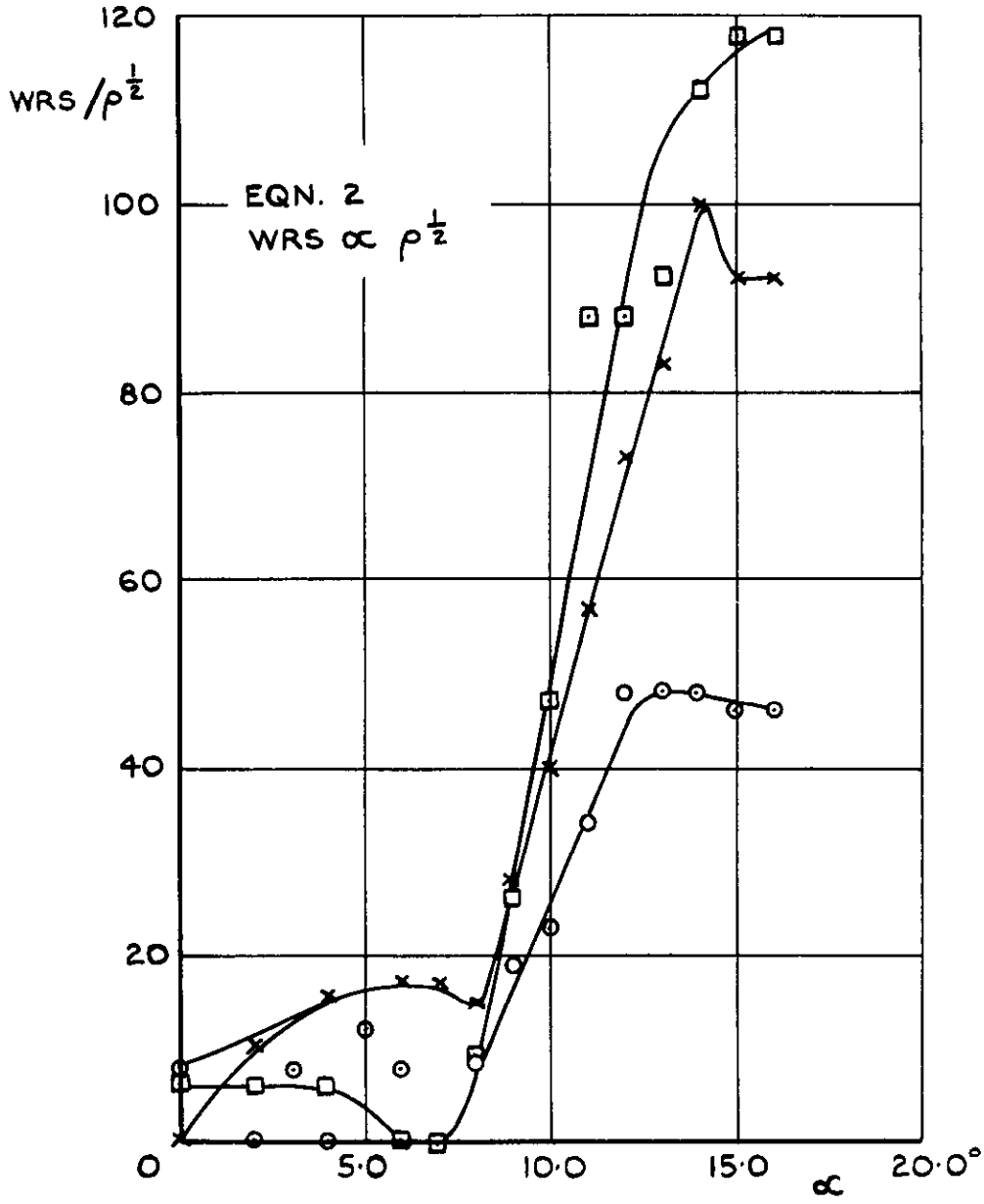

FIG.22 (b2) f = 380 C/S

FIG.22 (CONT'D) MODEL 4 COMPARISON OF BUFFETING SCALING RELATIONSHIPS FOR DIFFERENT MODES M=0·40

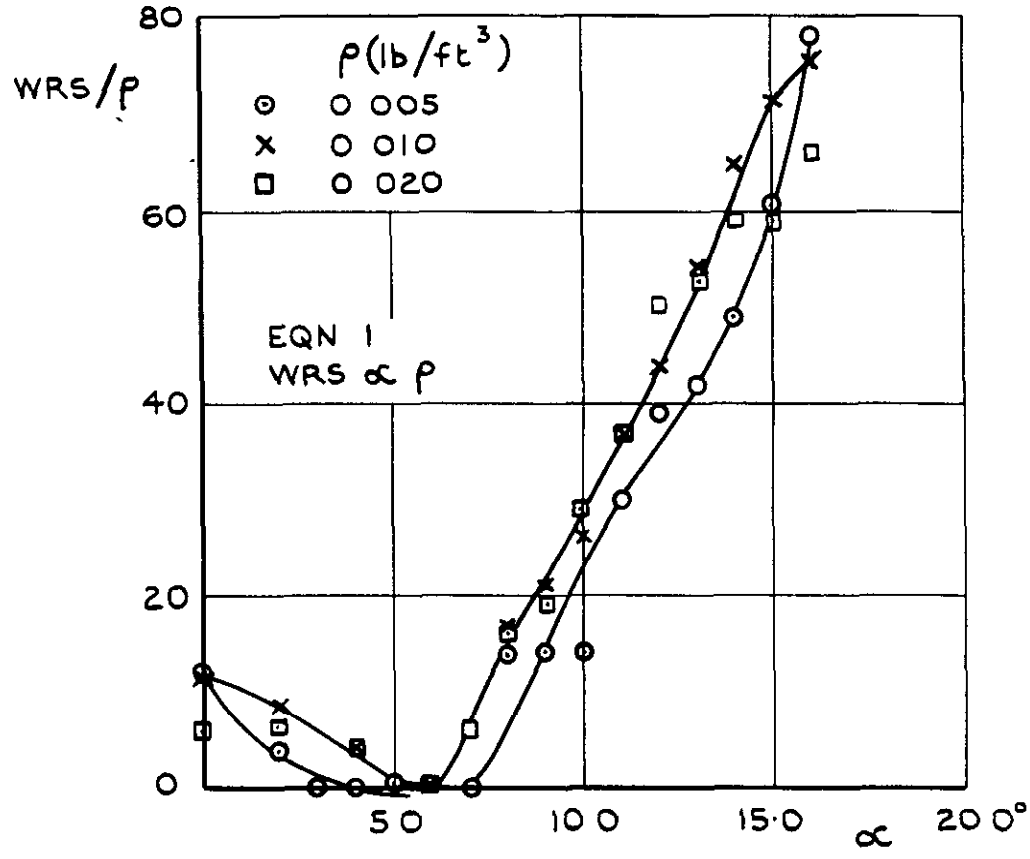

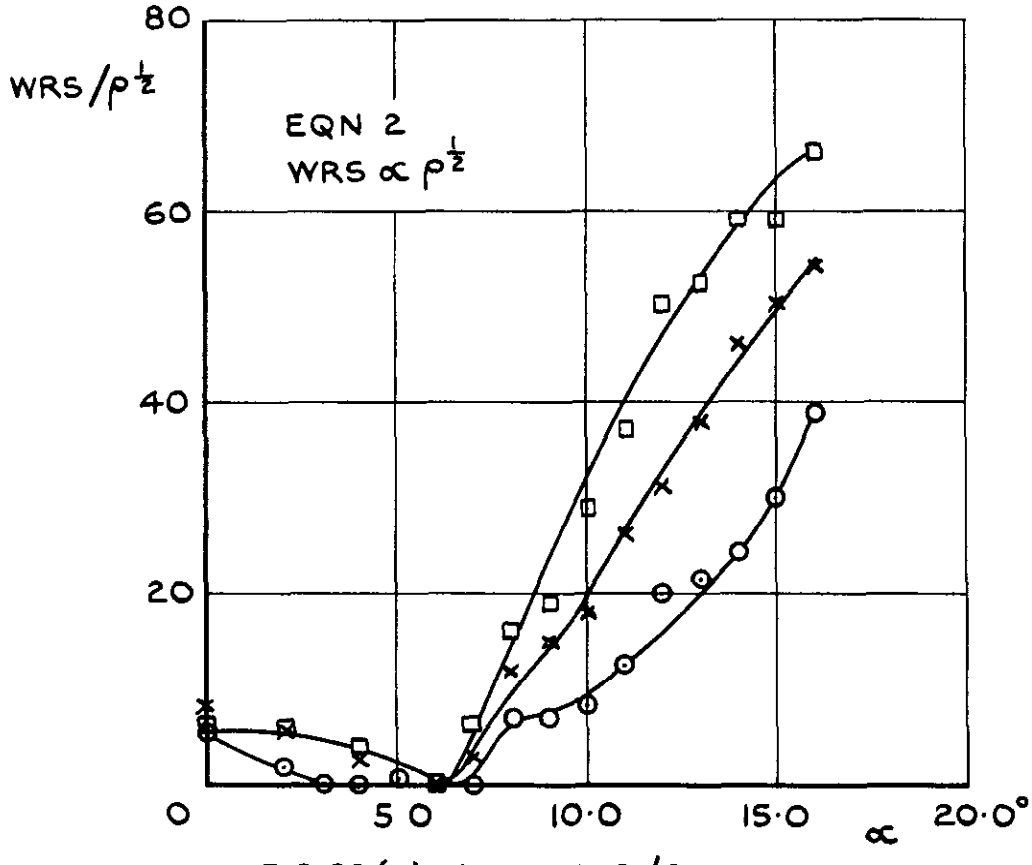

FIG 22 (c) f = 1470 c/s

FIG. 22 (CONCL'D) MODEL 4 COMPARISON OF BUFFETING SCALING RELATIONSHIPS FOR DIFFERENT MODES M = 0·40

Printed in England for Her Majesty's Stationery Office by the Royal Aircraft Establishment, Farnborough. Dd.125875. K.4

A.R.C. C.P. No.917
March 1966

Mabey, D.G.

533.6.013.43 :
533.693.3 :
532.527 :
533.6.011.32/34

MEASUREMENTS OF BUFFETING ON SLENDER WING MODELS

Tests on two solid slender wing models show that there are two stages in the wing buffeting at subsonic speeds;

(1) a mild buffeting due to leading-edge vortices, and

(2) a severe buffeting at vortex breakdown.

At supersonic speeds the mild buffeting is weaker, probably because of the reduced size and intensity of the leading-edge vortices.

P.T.O.

A.R.C. C.P. No.917
March 1966

Mabey, D.G.

533.6.013.43 :
533.693.3 :
532.527 :
533.6.011.32/34

MEASUREMENTS OF BUFFETING ON SLENDER WING MODELS

Tests on two solid slender wing models show that there are two stages in the wing buffeting at subsonic speeds;

(1) a mild buffeting due to leading-edge vortices, and

(2) a severe buffeting at vortex breakdown.

At supersonic speeds the mild buffeting is weaker, probably because of the reduced size and intensity of the leading-edge vortices.

P.T.O.

A.R.C. C.P. No.917
March 1966

Mabey, D.G.

533.6.013.43 :
533.693.3 :
532.527 :
533.6.011.32/34

MEASUREMENTS OF BUFFETING ON SLENDER WING MODELS

Tests on two solid slender wing models show that there are two stages in the wing buffeting at subsonic speeds;

(1) a mild buffeting due to leading-edge vortices, and

(2) a severe buffeting at vortex breakdown.

At supersonic speeds the mild buffeting is weaker, probably because of the reduced size and intensity of the leading-edge vortices.

P.T.O.

DETACHABLE ABSTRACT CARDS

Tests on two aeroelastic models at subsonic speeds show that the mild buffeting is principally at the wing 3rd or higher distortion modes. The order of magnitude of this buffeting suggests that on a supersonic transport aircraft this might be perceptible during subsonic climb-out at high EAS.

Tests on two aeroelastic models at subsonic speeds show that this mild buffeting is principally at the wing 3rd or higher distortion modes. The order of magnitude of this buffeting suggests that on a supersonic transport aircraft this might be perceptible during subsonic climb-out at high EAS.

Tests on two aeroelastic models at subsonic speeds show that the mild buffeting is principally at the wing 3rd or higher distortion modes. The order of magnitude of this buffeting suggests that on a supersonic transport aircraft this might be perceptible during subsonic climb-out at high EAS.

Published by
HER MAJESTY'S STATIONERY OFFICE
To be purchased from
49 High Holborn, London W C 1
423 Oxford Street, London W 1
13A Castle Street, Edinburgh 2
109 St Mary Street, Cardiff
Brazennose Street, Manchester 2
50 Fairfax Street, Bristol 1
35 Smallbrook, Ringway, Birmingham 5
80 Chichester Street, Belfast 1
or through any bookseller

S O CODE No. 23-9017-17